ELSEVIER

International Journal of Mass Spectrometry 193 (1999) 205–226

International Journal of Mass Spectrometry

Probing the interaction of alkali and transition metal ions with bradykinin and its des-arginine derivatives via matrix-assisted laser desorption/ionization and postsource decay mass spectrometry

Blas A. Cerda, Leticia Cornett[1], Chrys Wesdemiotis*

Department of Chemistry, University of Akron, Akron, OH 44325, USA

Received 5 April 1999; accepted 16 July 1999

Abstract

The complexes of the peptides (Pep) bradykinin (RPPGFSPFR), des-Arg^1-bradykinin, and des-Arg^9-bradykinin with the metal (M) ions Na^+, K^+, Cs^+, Cu^+, Ag^+, Co^{2+}, Ni^{2+}, and Zn^{2+} are generated in the gas phase by matrix-assisted laser desorption/ionization and the structures of the corresponding $[Pep + M^+]^+$ or $[Pep - H^+ + M^{2+}]^+$ cations are probed by postsource decay (PSD) mass spectrometry. The PSD spectra depend significantly on the metal ion attached; moreover, the various metal ions respond differently to the presence or absence of a basic arginine residue. The Na^+ and K^+ adducts of all three peptides mainly produce N-terminal sequence ions upon PSD; the fragments observed point out that these metal ions are anchored by the PPGF segment and not the arginine residue(s). In contrast, the adducts of Cu^+ and Ag^+ show a strong dependence on the position of Arg; complexes of des-Arg^1-Pep (which contains a C-terminal Arg) produce primarily y_n ions whereas those of des-Arg^9-Pep generate exclusively a_n and b_n ions. These trends are consistent with Cu^+ ligation by Arg's guanidine group. The $[Pep + Cs^+]^+$ ions mainly yield Cs^+; a second significant fragmentation occurs only if a C-terminal arginine is present and involves elimination of this arginine's side chain plus water. This reaction is rationalized through a salt bridge mechanism. The most prominent PSD products from $[Pep - H^+ + Co^{2+}]^+$ and $[Pep - H^+ + Ni^{2+}]^+$ contain at least one phenylalanine residue, revealing a marked preference for these divalent metal ions to bind to aromatic rings; the fragmentation patterns of the complexes further suggest that Co^{2+} and Ni^{2+} bind to deprotonated amide nitrogens. The coordination chemistry of Zn^{2+} combines features found with the divalent Co^{2+}/Ni^{2+} as well as the monovalent Cu^+/Ag^+ transition metal ions. Generally, the structure and fragmentation behavior of each complex reflects the intrinsic coordination preferences of the corresponding metal ion. (Int J Mass Spectrom 193 (1999) 205–226) © 1999 Elsevier Science B.V.

Keywords: Metalated bradykinins; Alkali versus transition metal ion coordination of peptides; Postsource decay; Metal ion attachment sites; Salt bridges

* Corresponding author. E-mail: wesdemiotis@uakron.edu

[1] Mailing address: Bruker Daltonics, Billerica, MA 01821.

PII S1387-3806(99)00164-5

1. Introduction

The biological activity of peptides and proteins is often mediated by conformational changes induced by the binding of metal ions. Metal ion–peptide/protein interactions are generally specific and greatly influenced by the amino acid composition of the metal-binding domains [1,2]. For example, Zn^{2+}, Cu^{2+}, Cu^{+}, Co^{2+}, Ni^{2+}, or Fe^{2+} preferentially bind at sites rich in histidine, cysteine, or methionine residues, whereas Ca^{2+}, Mg^{2+}, Na^{+}, or K^{+} predominantly interact with oxygen-rich sites containing aspartate and glutamate residues [1,2]. This selectivity is primarily determined by the binding strength of the metal ion to the ligands present in a particular domain of the host peptide/protein, but can also be affected by solvent molecules [1,2]. It is, therefore, of interest to study the gas phase interactions between metal ions and peptides or proteins to elucidate the intrinsic factors governing metal ion selection by such biomolecules.

Considerable work has so far been devoted to the gas phase unimolecular chemistry of alkali metal ion-bound peptides formed by fast atom bombardment (FAB) or electrospray ionization (ESI) [3–22]. On the basis of collisionally activated dissociation (CAD), labeling experiments, and theory, these studies have suggested several potential attachment sites for the metal ion, including the most basic group of the peptide (N-terminus or side chain) [3,21], the carbonyl O atoms [4,7,8,11–13], the carboxylate function of the zwitterionic peptide [5,6], or a combination thereof [7,8,21]. The lack of a general binding scheme has been attributed partly to the fact that the preferred binding site depends on the amino acid composition, thereby varying among different peptides [21], and partly to the mobility of alkali metal ions during CAD [22]. Two common CAD characteristics of alkali metal ion-coordinated peptides are their efficient backbone fragmentation (similar to protonated peptides) as well as the proclivity for a specific rearrangement at the C-terminus yielding a new, truncated peptide without the C-terminal residue (the so called $[b + M + OH]^{+}$ ion [6,10,14]).

The gas phase chemistry of transition metal ion-coordinated peptides has also been studied extensively [23–32]. Gross and co-workers reported the CAD spectra of singly charged peptide–transition metal complexes of the type $[Pep - H^{+} + M^{2+}]^{+}$ and $[Pep - 3H^{+} + M^{2+}]^{-}$, produced by FAB (M = Co, Ni, Mn, Fe) [25,28]. In cationic $[Pep - H^{+} + M^{2+}]^{+}$, aromatic side chains direct the fragmentation towards a_n ions that contain the aromatic residue [28]. Similarly, $[Pep - H^{+} + Fe^{2+}]^{+}$ complexes containing cysteine give rise to abundant a_n ions, n being the position of the cysteine residue [32]. Anionic $[Pep - 3H^{+} + M^{2+}]^{-}$ complexes fragment at the C-terminus by loss of CO_2 and H_2CO_2, at the N-terminus to form y_n and x_n sequence ions, and by loss of elements of the side chain if it is functionalized [25]. Adams and co-workers investigated the metastable dissociations of FAB-generated $[Pep - 3H^{+} + M^{2+}]^{-}$ complexes with Co^{2+} and Ni^{2+} [26]; such anions from tetra and larger peptides primarily yield N-terminal *b*- or *a*-type ions, suggesting metal ion coordination near the N-terminus, in analogy to solution chemistry. Parallel trends were observed for the metastable dissociation of doubly charged $[Pep + M]^{2+}$ complexes (M = Co, Ni, Cu, Zn), formed by ESI, which mainly produce *b*-type ions [27]. Hu and Loo [29] demonstrated that doubly charged electrosprayed complexes of histidine containing peptides with Zn^{2+}, Ni^{2+}, or Co^{2+} dissociate at the histidine sites upon CAD, whereas Cu^{2+} complexes show additional fragmentations by loss of CO_2 and the production of C-terminal fragment ions. Siu and co-workers [30] presented the ESI-CAD spectra of Ag^{+}-cationized di-, tri-, and oligopeptides with and without methionine, which is the Ag^{+} attachment site in solution; based on the dominance of N-terminal fragments in all spectra, it was concluded that the gas phase and solution structures of $[Pep + Ag]^{+}$ are different.

Fewer studies exist on metal ion-bound peptides produced by matrix-assisted laser desorption/ionization (MALDI) [31,33–41], and those reported have been mainly concerned with the detection of intact complexes formed in solution [31,33,34,36–40]. Information about the structures and dissociations of MALDI-produced metalated peptides is scarce [41]. Here, we report the unimolecular chemistry of such

complexes, as assessed by their postsource decay (PSD) tandem mass spectra [42]. The complexes studied are composed of the peptides bradykinin, des-Arg^1-bradykinin, or des-Arg^9-bradykinin and the metal ions Na^+, K^+, Cs^+, Cu^+, Ag^+, Co^{2+}, Ni^{2+}, or Zn^{2+}. These choices provide the opportunity to evaluate the effect of C- versus N-terminal basic residues on the interaction of peptides with various main group versus transition metal ions.

2. Methods

All mass spectra were acquired using a Bruker REFLEX III time-of-flight (TOF) mass spectrometer (Bruker Daltonics, Billerica, MA) equipped with a pulsed (3 ns pulse width) UV (337 nm) nitrogen laser for MALDI, a single-stage grid-less pulsed extraction ion source, a gated deflector (ion preselector) for MS/MS, a two-stage grid-less reflector, and two dual-microchannel plate detectors, one situated at the end of the first field-free region (space between the ion source exit and the reflector entrance) for detection in the linear mode and the other located at the end of the second field-free region (space between the reflector and the detector) for detection in the reflector mode. The experiments were performed in the reflector mode with the ion source acceleration potential held at 25 keV and the final reflector lens at 26.5 keV.

PSD spectra were acquired by tuning the ion preselector to transmit only the desired metal ion/peptide complex (complete isotopic cluster) and by recording the fragments formed from this ion in the first field-free region at each of 14 decreasing reflector voltage intervals. The resulting 14 mass spectral segments were pasted in-line by using the FAST algorithm provided by Bruker. For all spectra, the laser power was maintained slightly above the threshold required to produce ions and was increased only if product ion intensity significantly diminished. Prior to measuring a PSD spectrum, the mass scale of the reflector mode was calibrated using the protonated peptides Angiotensin I (M_r 1296.5) and ACTH 18–39 (M_r 2465.7). Mass calibration at each PSD spectral segment was performed automatically by Bruker's spectral pasting algorithm using ACTH 18–39 as calibrant. The mass accuracies were generally within 0.05%.

Stock solutions of the peptides (50–100 pmol/μL) and the α-cyano-4-hydroxycinnamic acid matrix (saturated) were prepared in water/acetonitrile (70:30 v/v) containing 0.1% trifluoroacetic acid. Peptide/matrix solutions were prepared by dissolving 1 μL of the peptide stock into 9 μL of the saturated matrix solution. For the formation of metal ion complexes, the peptide/matrix solutions were doped with approximately 0.3–0.5 μL of a 0.1 mg/ml solution of the appropriate metal ion acetate (in the same solvent). A moderate increase of the metal salt concentration led to the addition of several (2–4) metal ions, whereas higher concentrations of the metal salt mainly generated metal ion adducts of the matrix and barely any metalated peptide. The peptides were purchased from Sigma (St. Louis, MO); acetonitrile, α-cyano-4-hydroxycinnamic acid, trifluoroacetic acid, and the metal ion acetate salts were obtained from Aldrich (Milwaukee, WI).

3. Results and discussion

The MALDI-TOF mass spectra acquired (reflectron mode) were dominated by $[Pep + H]^+$ ions. The intensity of the metalated bradykinins ranged from 20% to 70% of the corresponding $[Pep + H]^+$ intensity, with Cu^+ and Ag^+ producing the strongest adduct signals, followed by Na^+ and K^+, then Cs^+, Co^{2+}, and Ni^{2+}, and finally Zn^{2+}. During PSD, the fragmentation efficiency was found to be higher for $[Pep + M^+]^+$ than $[Pep - H^+ + M^{2+}]^+$ complexes.

The PSD spectra of the twenty-four different complexes studied are presented in Figs. 1–8. The main sequence ions formed are labeled on the spectra, while all other identified products are marked by numbers which are described in the corresponding figure legends. Within each figure, ions of the same composition carry the same number. The Roepstorff and Fohlman nomenclature [43] is used as later modified by Biemann and co-workers [44].

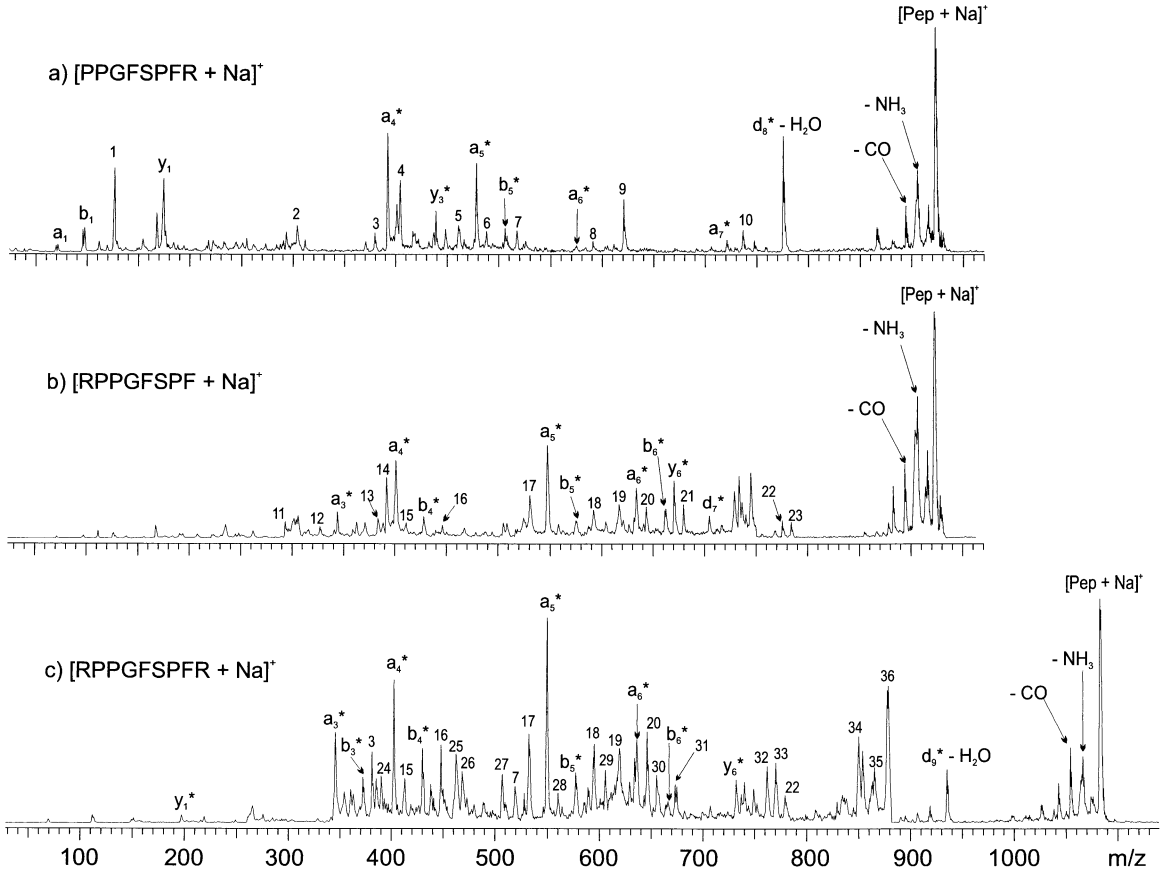

Fig. 1. PSD spectra of Na^+ complexes; (a) [des-Arg[1]-bradykinin + Na]$^+$, (b) [des-Arg[9]-bradykinin + Na]$^+$, and (c) [bradykinin + Na]$^+$. Peaks labeled with numbers correspond to: 1, $[PG + Na - H_2O - CO]^+$; 2, $[y_2 - NH_3]$; 3, $[y_3^* - 60]$; 4, $[y_3^* - NH_3 - H_2O]$; 5, $[a_5^* - H_2O]$; 6, $[b_5^* - H_2O]$; 7, $[FSPF + Na]^+$; 8, $[b_6 + Na + OH - CH_2O]$; 9, $[b_6 + Na + OH]$; 10, $[b_7 + Na + OH - CH_2O]$; 11, $[b_2 + Na + OH]$; 12, $[a_3^* - NH_3]$; 13, $[a_4^* - NH_3]$; 14, $[PGFS + Na - 2H_2O]^+$; 15, $[b_4^* - NH_3]$; 16, $[b_4 + Na + OH]$; 17, $[a_5^* - NH_3]$; 18, $[b_5 + Na + OH]$; 19, $[a_6^* - NH_3]$; 20, $[b_6^* - H_2O]$; 21, $[b_6 + Na + OH]$ (ions #9 and 21 have different sequences); 22, $[b_7 + Na + OH]$; 23, $[y_7^* + NH_3]$; 24, $[b_3 + Na + OH]$; 25, $[PPGFS + Na - 2H_2O - CO]^+$; 26, $[y_4^* - 60]$; 27, $[a_5^* - HN{=}C{=}NH \text{ or } C_3H_6]$; 28, $[b_5^* - NH_3]$; 29, $[PPGFSP + Na - H_2O]^+$; 30, $[y_5^* - 2H - H_2O]$; 31, $[y_5^* - 2H]$; 32, $[b_7 + Na + OH - H_2O]$; 33, $[PPGFSPF + Na]^+$; 34, $[a_8^* - CH_2O]$; 35, $[a_8^* - NH_3]$; 36, $[b_8^* - CH_2O]$. Note that small caps (as in b_6) represent protonated sequence ions [43,44], whereas small caps *with* an asterisk (as in b_6^*) abbreviate metalated ions.

3.1. PSD of [Pep + Na]$^+$, [Pep + K]$^+$, and [Pep + Cs]$^+$ ions

The PSD spectrum of the Na^+ adduct of des-arg[1]-bradykinin, $[PPGFSPFR + Na]^+$, is shown in Fig. 1(a). This complex generates mainly N-terminal $[a_n - H + Na]^+$ and $[b_n - H + Na]^+$ ions but very few C-terminal $[y_n - H + Na]^+$ fragments; for brevity, these and related sequence ions will be termed a_n^*, b_n^*, y_n^*, etc. (the asterisk symbolizing metal ion content). Two important PSD features are the formation of $[b_n + Na + OH]^+$-type (peaks #8, 9, 10) and of $[y_3^* - 60]^+$ ions (#3); the former are diagnostic of sodiated peptides (vide supra) [6–8,10–12,14], whereas a 60 u neutral loss from *y*-type (or molecular) ions of alkali cationized peptides has been shown to be indicative of a C-terminal arginine residue [14]. Another unique characteristic of the spectrum is the presence of a $[d_8^* - H_2O]^+$ fragment ion which formally arises from $a_8^* + 1$ via loss of

parts of the arginine and serine side chains (148 u) [44]; its formation mechanism will be discussed in more detail later. Aside from the mentioned $[y_3^* - 60]^+$ ion, the only other sodiated C-terminal fragment ions observed are y_3^* and $[y_3^* - NH_3 - H_2O]^+$ (peak #4). Evidently, despite the presence of a C-terminal Arg in des-Arg^1-bradykinin, the corresponding [des-Arg^1-Pep + Na]$^+$ ion preferably yields N-terminal fragment ions.

The PSD spectrum of sodiated des-arg^9-bradykinin, [RPPGFSPF + Na]$^+$, is similarly dominated by N-terminal a_n^* and b_n^* sequence ions, cf. Fig. 1(b); the only C-terminal fragment observed is y_6^*. Placement of the arginine residue at the N-terminus enhances, however, the formation of $[b_n + Na + OH]^+$ fragments, now leading to an almost complete series (peaks #11, 16, 18, 21, 22). Further, the absence of $[y_n^* - 60]^+$, $[y_n^* - NH_3 - H_2O]^+$, and $[d_8^* - H_2O]^+$ ions corroborates that such products are characteristic of a C-terminal arginine residue. On the other hand, the N-terminal Arg residue promotes the formation of $[a_n^* - NH_3]^+$ ions (#12, 13, 17, 19).

The PSD spectrum of sodiated bradykinin, [RPPGFSPFR + Na]$^+$, shown in Fig. 1(c), exhibits features that are a blend of those found in Fig. 1(a) and (b). In analogy to the des-Arg^1-bradykinin complex, sodiated bradykinin produces $[y_{3,4}^* - 60]^+$ (#3, 26) as well as $[d_9^* - H_2O]^+$ fragment ions. Additionally, almost complete series of a_n^*, b_n^*, and $[b_n + Na + OH]^+$ (#24, 16, 18, 22) are observed, as is the case for des-Arg^9-bradykinin. Although both N- and C-terminal product ions are included in Fig. 1(c), it is evident that the N-terminal a_n^* and b_n^* ions predominate. In fact, the major sequence ions from all three sodiated peptides are a_n^* ions (Fig. 1), indicating that the C-terminal arginine is not a likely binding site for Na^+. The formation of almost complete series of a- and b-type ions suggests, instead, a close association of the metal ion with the backbone carbonyl O atoms.

In all three PSD spectra of Fig. 1, a_4^* and a_5^* are among the 2–3 most abundant fragment ions. With bradykinin and des-Arg^9-bradykinin, these fragment ions are identical in *m/z* and composition, including Arg, Pro, Gly, and Phe residues in the sequences RPPG for a_4^* and RPPGF for a_5^*. With des-Arg^1-bradykinin, a_4^* and a_5^* contain Pro, Gly, Phe, and Ser residues in the sequences PPGF and PPGFS, respectively. The sequence PPGF, which is present in a_5^* from bradykinin and its des-Arg^9 analog as well as and in a_4^* and a_5^* from des-Arg^1-bradykinin, thus, provides a favorable coordination environment for Na^+. The sequence RPPG, contained in a_4^* from bradykinin and des-Arg^9-bradykinin, appears to offer a comparably adequate anchoring point for the metal ion. These data are consistent with Na^+ attachment near the N-terminus and participation of the N-terminal arginine (when present) in the binding of Na^+.

Substantiating evidence for this conclusion comes from theoretical calculations by Bowers and coworkers who performed a detailed molecular mechanics/dynamics study on the structures of [bradykinin + Na]$^+$ [38]. It was found that the most stable conformer has octahedral coordination for Na^+, involving the guanidine group of R^1, the carbonyl oxygens of P^2 and P^3, the F^5 carbonyl oxygen and phenyl ring, and a weak interaction with the R^9 guanidine side chain (Scheme 1). Our previously described findings are in excellent agreement with such a structure in which four of the six Na^+ ligands are provided by the PPGF segment.

The PSD spectra of the [Pep + K]$^+$ adducts of des-Arg^1-, des-Arg^9-, and bradykinin are shown in Fig. 2(a), (b), and (c), respectively. In general, they show strong similarities to the corresponding spectra of the [Pep + Na]$^+$ complexes; in both cases, N-terminal *a*- and *b*-type ions are dominant, and most of the discussion given for the [Pep + Na]$^+$ adducts applies also to the corresponding [Pep + K]$^+$ systems. A noticeable difference is the markedly larger abundance of $[b_6 + K + OH]^+$ (#8) and $[b_6^* - H_2O]^+$ (#19) from potassiated des-Arg^1-bradykinin and des-Arg^9- or bradykinin, respectively (Fig. 2), compared to the abundances of the corresponding sodiated ions (Fig. 1). All of these b_6-type ions contain the amino acid sequence PPGFS, which is closely related to the preferred binding domain for Na^+ (PPGF), in keeping with the similar chemical properties of these two metal ions. The larger ionic radius of K^+ allows, however, this metal ion to

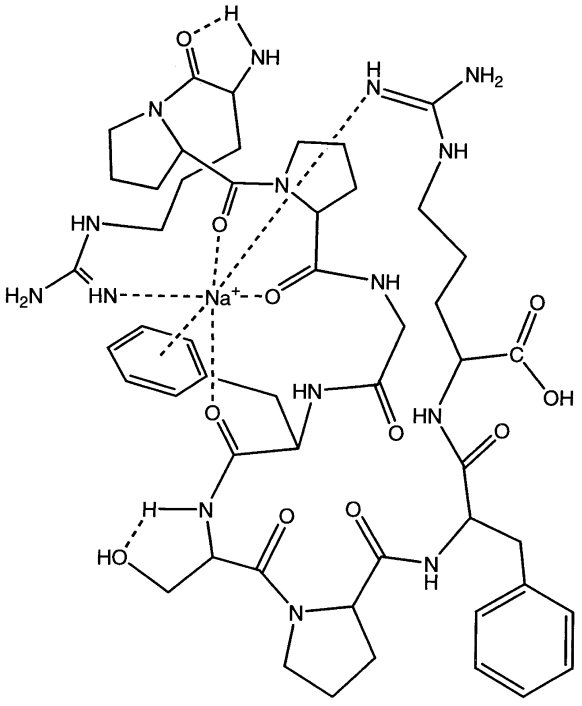

Scheme 1.

accommodate additional and/or more distant ligands, justifying the increased abundance of b_6-type ions from the K^+- vis à vis the Na^+-bound peptides.

It is noteworthy that both the Na^+ and K^+ complexes also form internal fragment ions, especially with bradykinin. The following internal fragments could be identified in the PSD spectra of Figs. 1 and 2: $[FSPF + Na]^+$ with des-Arg^1-Pep (#7); $[PGFS + Na - 2H_2O]^+$ (*b*-type minus H_2O; #14) and $[FSPF + K]^+$ (#14) with des-Arg^9-Pep; and $[PPGFS + Na - 2H_2O - CO]^+$ (*a*-type minus H_2O; #25), $[FSPF + Na]^+$ (#7), $[PPGFSP + Na - H_2O]^+$ (*b*-type minus H_2O; #29), $[PPGFSPF + Na]^+$ (#33), $[FSPF + K]^+$ (#14), and $[PPGFSPF + K]^+$ (#24) with bradykinin. Although these internal ions are not among the most prominent fragments, their generation confirms that Na^+ and K^+ bonds to the terminal arginine residue(s) are not very strong and that the backbone carbonyl groups (along with the Phe and Ser side chains) can offer a variety of comparable coordination environments to these metal ions. A similar coordination chemistry (viz. preference for the backbone carbonyl and specific side chain groups) has been observed upon CAD of the Ca^{2+} adducts of peptides that contain motifs for Ca^{2+} binding sites in proteins [45].

In dramatic contrast to the sodiated and potassiated complexes, the Cs^+ adducts of des-Arg^1-, des-Arg^9- and bradykinin give very simple PSD spectra, containing only one or two dominant fragment ions (Fig. 3). As pointed out by several investigators [3,10,11,16], when alkali metal ion-bound peptides dissociate, the formation of metalated fragments competes with the ejection of the metal ion. Due to the decreasing metal ion–ligand binding strength with increasing ionic radius, smaller cations (Li^+, Na^+, and K^+) mainly produce metalated sequence ions, whereas larger cations (Rb^+ and Cs^+) favorably detach as bare metal ions. For this reason, formation of Cs^+ by loss of the intact neutral peptide is a (or the) major PSD process for the Cs^+ adducts of all three peptides studied here (Fig. 3). With the exception of [des-Arg^9-bradykinin + Cs]$^+$, which only shows additional low intensity peaks (a_5^*, b_5^*, $[b_6^* - H_2O]^+$, y_6^*), [des-arg^1-bradykinin + Cs]$^+$ and [bradykinin + Cs]$^+$ undergo a competitive process, giving rise to the fragments $[d_8^* - H_2O]^+$ and $[d_9^* - H_2O]^+$, respectively, which are also notable in the PSD spectra of the corresponding Na^+ and K^+ adducts [cf. parts (a) and (c) in Figs. 1–3]. This process is specific to complexes possessing a C-terminal Arg residue. Further, the substantial abundance of $[d_n^* - H_2O]^+$ from the Cs^+-cationized peptides reveals that these fragments are formed via a low barrier dissociation which can efficiently compete with Cs^+ detachment.

d-Type sequence ions from metalated peptides are believed to originate from the corresponding $(a + 1)$-type radical ions by loss of a radical from the side chain of the C-terminal residue [10]. The $[d_8^* - H_2O]^+$ and $[d_9^* - H_2O]^+$ ions observed from [des-Arg^1-bradykinin + Cs]$^+$ and [bradykinin + Cs]$^+$, respectively, could thus arise via the stepwise decomposition $[Pep + Cs]^+ \rightarrow a_n^* + 1$ (loss of C-terminal $^{\cdot}COOH$) $\rightarrow d_n^*$ (loss of $CH_2CH_2NHC(NH_2)$=NH from Arg's side chain) $\rightarrow$

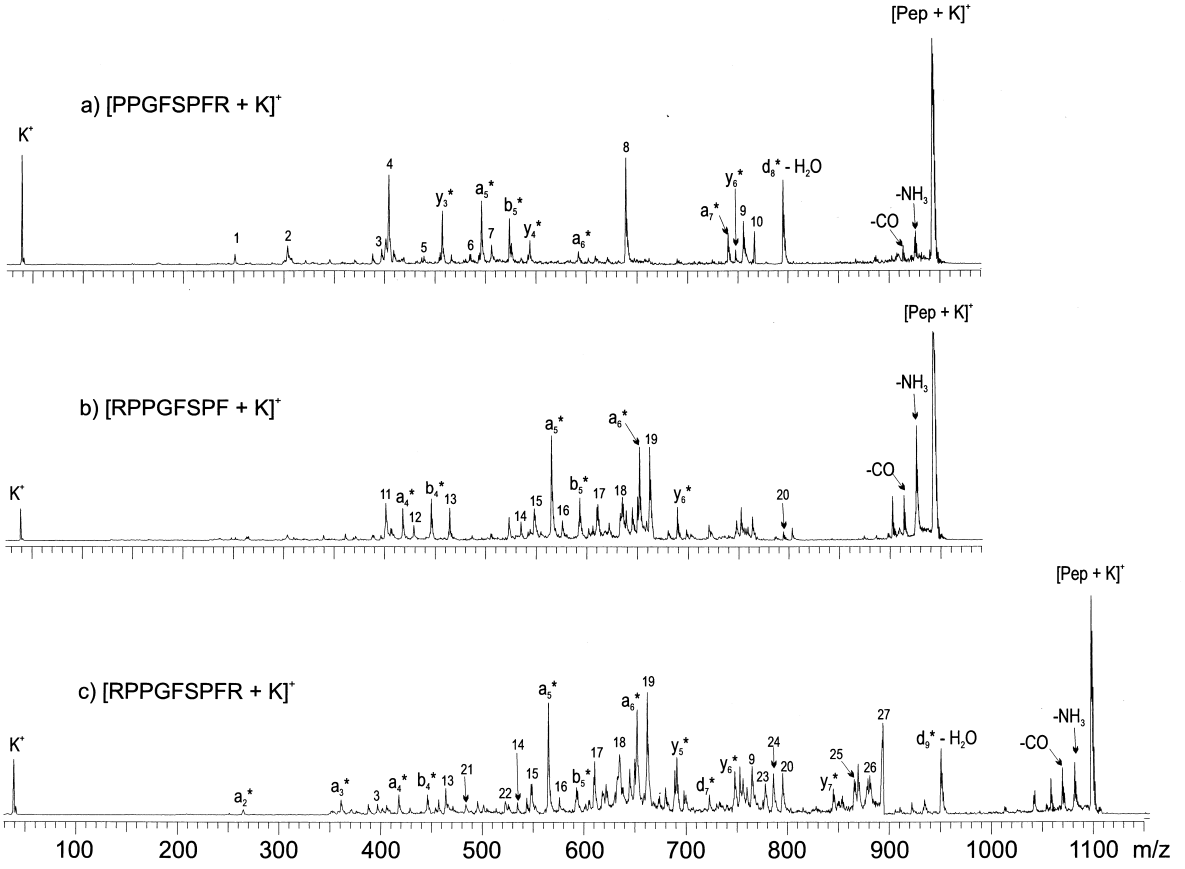

Fig. 2. PSD spectra of K^+ complexes; (a) [des-Arg^1-bradykinin + K]$^+$, (b) [des-Arg^9-bradykinin + K]$^+$, and (c) [bradykinin + K]$^+$. Peaks labeled with numbers correspond to: 1, [b_2 + K + OH]; 2, [y_2 − H_2O]; 3, [y_3^* − 60]; 4, [y_3^* − NH_3 − 2H_2O]; 5, [y_3^* − H_2O]; 6, [y_4^* − 60]; 7, [b_5^* − H_2O]; 8, [b_6 + K + OH]; 9, [b_7 + K + OH − CH_2O]; 10, [d_8^* − H_2O − CO]; 11, [a_4^* − NH_3]; 12, [b_4^* − NH_3]; 13, [b_4 + K + OH], 14, [FSPF + K]$^+$; 15, [a_5^* − NH_3]; 16, [b_5^* − NH_3]; 17, [b_5 + K + OH]; 18, [a_6^* − NH_3]; 19, [b_6^* − H_2O]; 20, [b_7 + K + OH]; 21, [y_4^* − 60]; 22, [a_5^* − HN=C=NH or C_3H_6]; 23, [b_7 + K + OH − H_2O]; 24, [PPGFSPF + K]$^+$; 25, [a_8^* − CH_2O]; 26, [a_8^* − NH_3]; 27, [b_8^* − CH_2O].

$[d_n^* - H_2O]^+$ (water loss from Ser's side chain). The absence of $a_n^* + 1$, d_n^*, and [Pep + Cs − H_2O]$^+$ ions in the PSD spectra of [des-Arg^1-bradykinin + Cs]$^+$ and [bradykinin + Cs]$^+$ makes, however, such a scenario unlikely.

A plausible alternative pathway to the observed $[d_n^* - H_2O]^+$ ions without the a priori production of $a_n^* + 1$ or d_n^* ions is proposed in Scheme 2. The key feature of this mechanism is a zwitterionic intermediate in which the deprotonated carboxylate end is simultaneously solvated by the protonated guanidine group of the C-terminal arginine, the hydroxyl group of serine, and the metal ion. The strong hydrogen bond between the carboxylate and hydroxyl groups can facilitate the elimination of water from serine to yield an ion–molecule complex between the carboxylate moiety and the H_2O molecule, where the negatively charged carboxylate group is more optimally solvated. Within this complex, cleavage of the $^-$OOC–C$^\alpha$ bond to release the stable CO_2 molecule can initiate the displacement of ethylene and guanidine, thereby producing $[d_n^* - H_2O]^+$ directly (Scheme 2) without having to proceed through $a_n^* + 1$ or d_n^* ions (which are not observed in the PSD

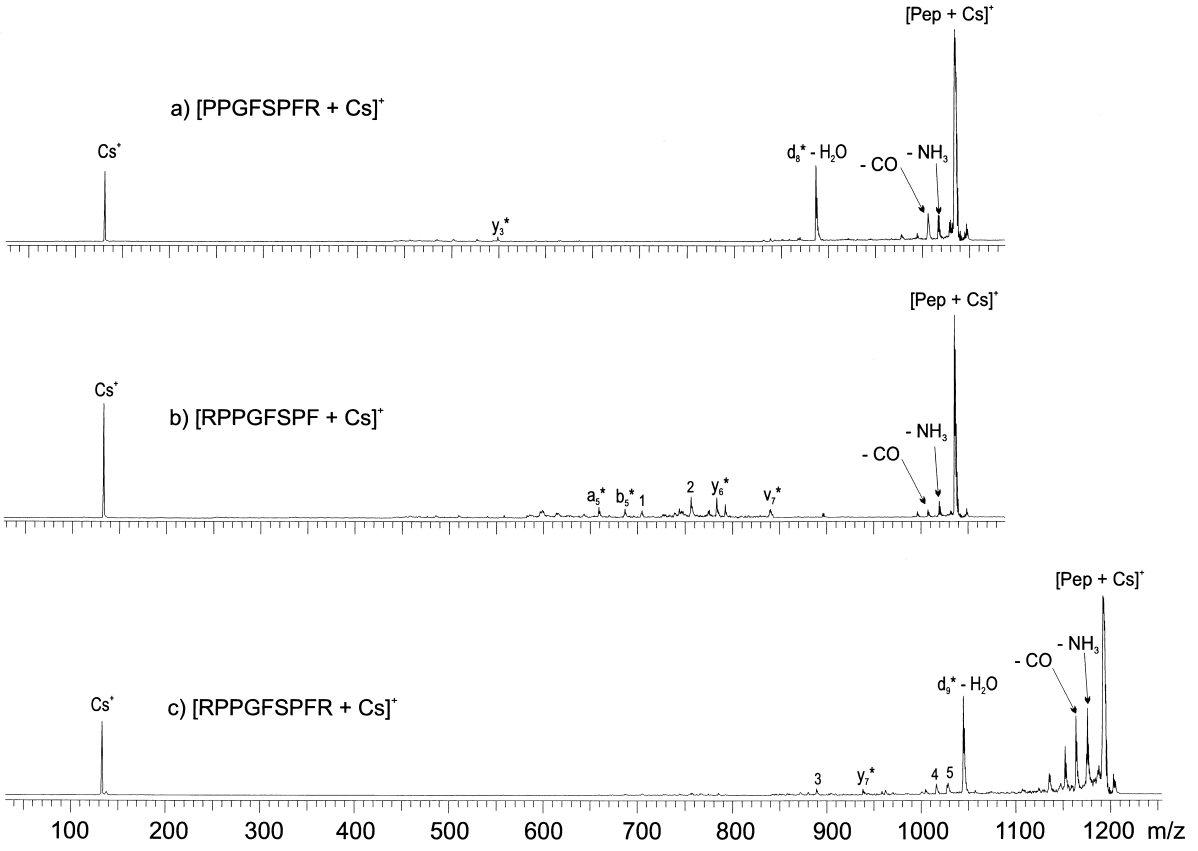

Fig. 3. PSD spectra of Cs^+ complexes; (a) [des-Arg^1-bradykinin + Cs]$^+$, (b) [des-Arg^9-bradykinin + Cs]$^+$, and (c) [bradykinin + Cs]$^+$. Peaks labeled with numbers correspond to: 1, [b_5 + Cs + OH]; 2, [b_6^* − H_2O]; 3, [b_7 + Cs + OH]; 4, [d_9^* − H_2O − CO]; 5, [d_9^* − H_2O − NH_3].

spectra). Such a mechanism justifies the specificity of $[d_n^* - H_2O]^+$ formation from bradykinins carrying a C-terminal arginine residue, which has been shown to readily adopt zwitterionic structures [41,46]. It is noticed from Figs. 1–3 that the relative proportion of $[d_n^* - H_2O]^+$ increases as the metal ion is changed from Na^+ to K^+ to Cs^+. This trend is attributed to an increasing stabilization of the zwitterionic intermediates in this direction; recent studies by Williams et al. [47] and Wesdemiotis and Cerda [48] have indicated that zwitterionic arrangements (salt bridges) within [arginine + alkali ion]$^+$ complexes become more stable with increasing radius of the metal ion.

3.2. PSD of [Pep + Cu]$^+$ and [Pep + Ag]$^+$ ions

The Cu^+ adduct of des-Arg^1-bradykinin, [PPGFSPFR + Cu]$^+$, gives rise to the PSD spectrum of Fig. 4(a), which is dominated by the C-terminal ions y_1^*, y_3^*, y_4^*, and y_5^*, as had also been reported by Shields et al. [41]. This finding indicates a strong interaction between Cu^+ and the peptide's C-terminal arginine residue, which is further substantiated by the large abundance of the arginine immonium ion [HN=CH$(CH_2)_3$NHC(NH_2)=NH + Cu]$^+$ (peak #2). In previous studies [49,50], we showed arginine to be the amino acid of highest Cu^+ affinity; it is, thus, not surprising that arginine is an important binding site

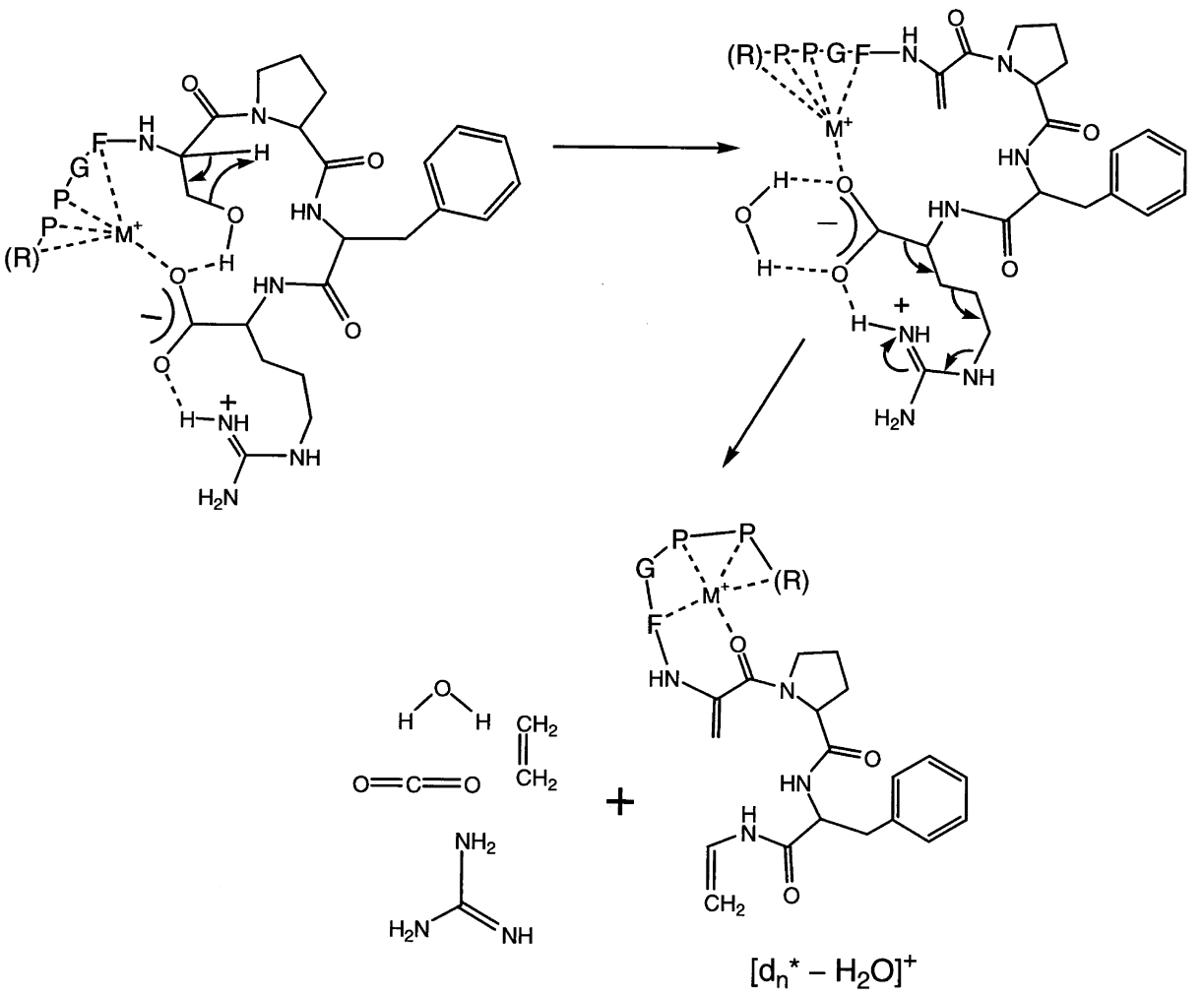

Scheme 2.

for Cu^+ within this peptide. The formation of low-intensity N-terminal a_n^* and b_n^* fragment ions reveals, however, that the N-terminal residues of the peptide contain moderately competitive binding sites for Cu^+ (at least in ions that have sufficient internal energy to dissociate).

Cu^+, a closed-shell d^{10} ion, prefers distorted tetrahedral or approximately trigonal coordination geometries [1,2]. The PSD data point out that the guanidine side chain furnishes one of the ligands. Based on the reported Cu(I) affinities of the amino acids present in the peptide [49–51], viz. G (269 kJ mol^{-1}) < S (282) < P (289) < F (302) < R (364), a phenylalanine residue (phenyl π electrons) is the most suitable choice for the second ligand, with the remaining 1–2 ligands provided by the amide carbonyls. In agreement with such expectations, the major C-terminal fragments y_3^*, y_4^*, y_5^*, and $[x_6^* - H_2O]^+$ (#6) bear both an Arg as well as a Phe residue [Fig. 4(a)]. Further, the high proportion of *y*-type ions agrees well with the presence of Cu^+–carbonyl interactions which would facilitate y_n^* generation by weakening the amide bond to be cleaved, as illustrated in Scheme 3 for y_3^*. The proposed mechanism involves a 1,4-hydrogen transfer from an amide nitrogen to the emerging N-terminus of the y_n^* ion, followed by

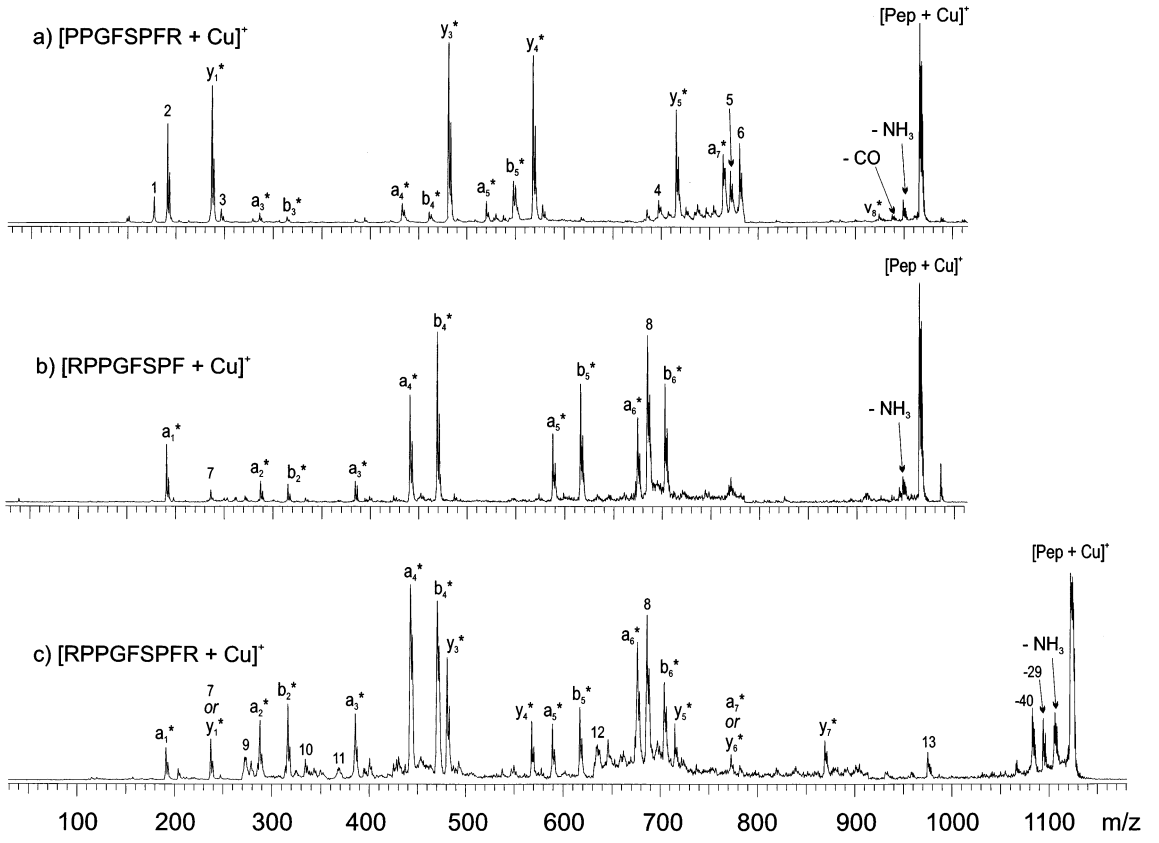

Fig. 4. PSD spectra of Cu^+ complexes; (a) [des-Arg^1-bradykinin + Cu]$^+$; (b) [des-Arg^9-bradykinin + Cu]$^+$; and (c) [bradykinin + Cu]$^+$. Peaks labeled with numbers correspond to: 1, [b_1 + Cu + OH]; 2, [HN=CH(CH$_2$)$_3$NHC(NH$_2$)=NH + Cu]$^+$; 3, [SP + Cu − H$_2$O]$^+$; 4, [y_5^* − H$_2$O]; 5, [y_6^* − 1]; 6, [x_6^* − H$_2$O]; 7, [b_1 + Cu + OH]; 8, [b_6^* − H$_2$O]; 9, [a_2^* − NH$_3$]; 10, [b_2 + Cu + OH]; 11, [a_3^* − NH$_3$]; 12, [b_5 + Cu + OH]; 13, [d_9^* − H$_2$O].

elimination of CO and an imine [25,52]. Such a reaction is less likely to occur at the C-terminal side of internal proline residues where there is no H atom at the amide nitrogen and H-transfer from more remote (entropically less favored) locations would be necessary; indeed, y_2^* and y_6^*, which would require cleavage at the PPGFSP–FR and PP–GFSPFR bonds, respectively, are minuscule or absent. Interestingly, y_7^* is also not observed (despite the presence of a N–H bond at the N-terminus), suggesting that five-membered ring H migrations over a proline ring are additionally subject to significant steric strain.

Placing the arginine residue at the C-terminus, i.e. binding Cu^+ to des-Arg^9-bradykinin ([RPPGFSPF + Cu]$^+$), dramatically changes the PSD spectrum which now displays exclusively N-terminal fragment ions [Fig. 4(b)]. The principal products are b_{4-6}^*, a_{4-6}^*, and [b_6^* − H$_2$O]$^+$ (#8). This profound change attests that arginine is again the primary anchoring point for Cu^+. As with the isomeric des-Arg^1 octapeptide, the other 2–3 ligands needed for the favored distorted tetrahedral or trigonal Cu^+ coordination most probably are a Phe residue (also present in all major fragments except b_4^*/a_4^*) and the amide groups. The complete absence of C-terminal fragments in the PSD spectrum of [des-Arg^9-bradykinin + Cu]$^+$ further points out that an N-terminal arginine forms a particularly stable bond with Cu^+.

Scheme 4 exemplifies the formation of *b*-type ions from [RPPGFSPF + Cu]$^+$ (for b_4^*), assuming an oxazolone product ion structure, which is true for

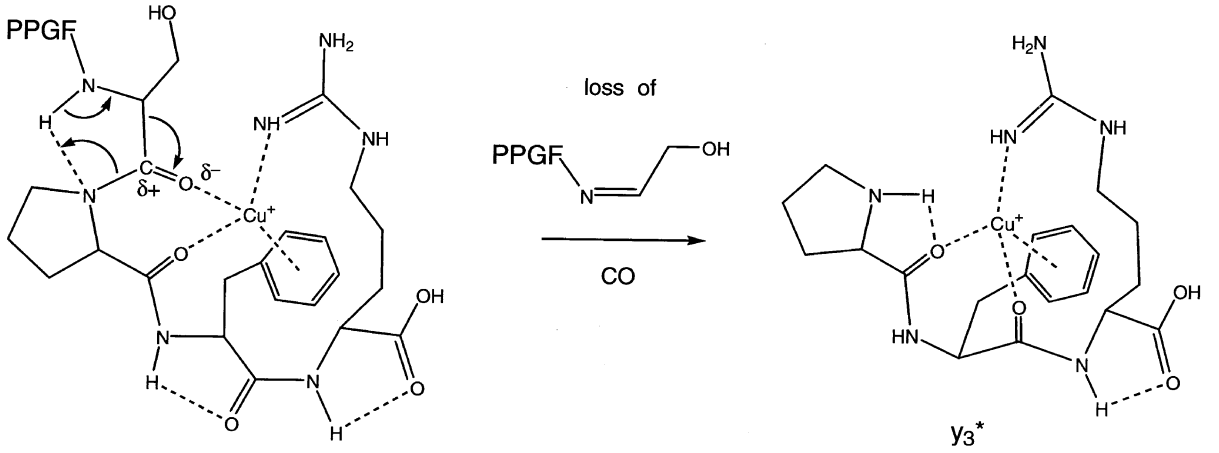

Scheme 3.

protonated [53] and silver containing [54] *b*-type fragment ions. Nucleophilic attack by a polarized carbonyl O atom onto the C-terminally adjacent carbonyl C atom initiates the formation of an oxazolone ring, which is completed by breakup of the amide bond to the attacked C atom and proton transfer to the incipient N-terminus of the neutral fragment (Scheme 4). The b_6^* fragment produced in an analogous pathway possesses a hydroxymethyl group in the oxazolone ring (at C atom #3), which could readily dehydrate to give a conjugated system; this, in turn, can account for the large intensity of $[b_6^* - H_2O]^+$ (peak #8) in Fig. 4(b).

[Bradykinin + Cu]$^+$, which has arginine residues at both termini, expectedly gives both N- and C-terminal fragment ions upon PSD, cf. Fig. 4(c). However, the N-terminal fragments are more abundant, with the almost complete a_n^* and b_n^* series

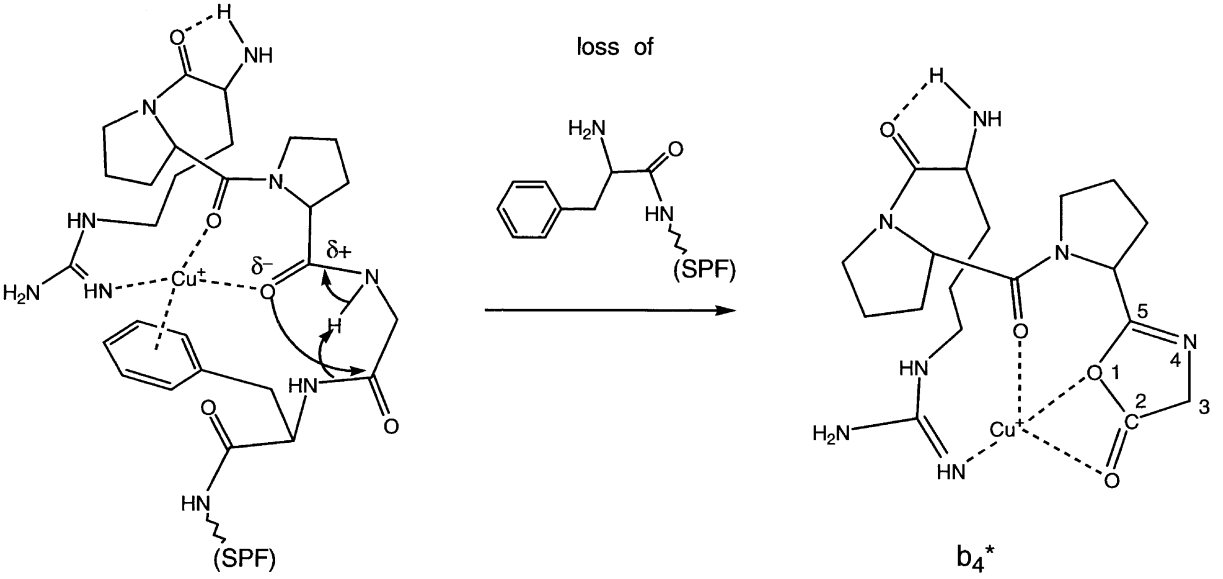

Scheme 4.

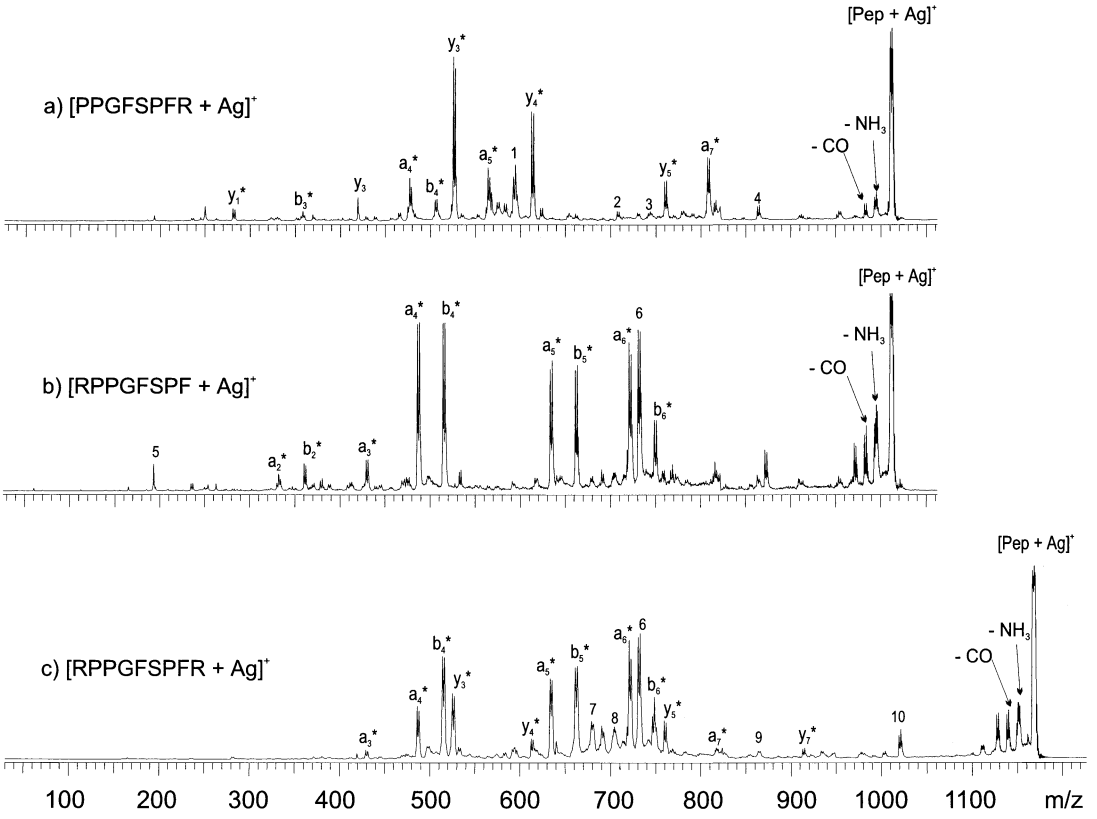

Fig. 5. PSD spectra of Ag^+ complexes; (a) [des-Arg^1-bradykinin + Ag]$^+$, (b) [des-Arg^9-bradykinin + Ag]$^+$, and (c) [bradykinin + Ag]$^+$. Peaks labeled with numbers correspond to: 1, [y_4^* − H_2O]; 2, [b_6 + Ag + OH]; 3, [y_5^* − H_2O]; 4, [d_8^* − H_2O]; 5, [a_2 − 2NH_3]; 6, [b_6^* − H_2O]; 7, [b_5 + Ag + OH]; 8, [a_6^* − NH_3]; 9, [b_7 + Ag + OH]; 10, [d_9^* − H_2O].

standing out in the spectrum. Note the striking resemblance of the PSD spectra of [des-Arg^9-Pep + Cu]$^+$ and [Pep + Cu]$^+$ [Fig. 4(b) and (c)] both of which show prominent a_{4-6}^*, b_{4-6}^*, and [b_6^* − H_2O]$^+$ (#8) fragments. This result indicates that the N-terminal arginine and nearby amino acids provide a superior coordination environment, as compared to the residues available at the C-terminus. Cu^+ binding at the N-terminus would allow the C-terminal arginine residue to become zwitterionic (via proton transfer from the carboxylate terminus to the guanidine group). That such a zwitterionic structure can be formed is attested by the appearance of a [d_9^* − H_2O]$^+$ fragment (#13) in the PSD spectrum of Fig. 4(c); as discussed earlier such a fragment ion is best rationalized via a zwitterionic intermediate (cf. Scheme 2).

Fig. 5(a), (b), and (c) present the PSD spectra of the [Pep + Ag]$^+$ adducts of des-Arg^1, des-Arg^9-, and bradykinin, respectively. Ag^+ and Cu^+ are both d^{10}-closed shell ions and have similar relative affinities to α-amino acids [49–51,55]; hence, their intrinsic coordination chemistries should be similar. This is confirmed by the almost identical PSD fragments from the [Pep + Ag]$^+$ and [Pep + Cu]$^+$ complexes of the three bradykinins studied (Figs. 4 and 5). For this reason, the discussion dedicated to [Pep + Cu]$^+$ also applies to the corresponding [Pep + Ag]$^+$ systems.

Unlike for Cu^+ and Ag^+, whose absolute or relative binding energies to α-amino acids are available, the thermochemistry of alkali metal ions to most amino acids remains unknown. According to the few existing data [56–58], Na^+ forms the weakest bond

with glycine (153 kJ mol^{-1} [57]) and the strongest with arginine (~200 kJ mol^{-1} [59]). This is also true for Cu^+, the Gly–Cu^+ and Arg–Cu^+ binding affinities being 269 and 364 kJ mol^{-1}, respectively [49–51]. Hence, Na^+ affinities are substantially lower than the corresponding Cu^+ affinities and vary less among different amino acids. This drastic difference in thermochemistry results in markedly distinct reactivities for a Na^+- versus Cu^+-bound peptide. Because Cu^+ is strongly attached to arginine residues, the position of such a residue within the sequence is important and determines the types of unimolecular reactions evolving upon activation of the complex. In sharp contrast, Na^+ is bound much weaker by arginine residues, both in absolute and relative terms. Here, the position of an arginine residue is less important, the dissociation behavior rather depending on what alternative, better coordination sites exist in the peptide; in the bradykinins studied, the PPGF motif appears to be the alternative, superior binding site. This site is common to all three bradykinins, leading to several common major fragments from the respective sodiated complexes (vide supra).

3.3. PSD of $[Pep - H + Co]^+$ and $[Pep - H + Ni]^+$ ions

Divalent Co^{2+} (d^7) and Ni^{2+} (d^8) are borderline Lewis acids and both prefer binding to aromatic rings and negatively charged nitrogen atoms in distorted octahedral geometries [2]. Accordingly, it is not surprising that the intrinsic reactivities of the complexes $[Pep - H^+ + Co^{2+}]^+$ and $[Pep - H^+ + Ni^{2+}]^+$ are found to be very similar. In what follows, these ions are described as $[Pep - H + M]^+$ (M = Co^{2+} or Ni^{2+}) and their PSD spectra are discussed jointly, pointing out significant differences when appropriate. It is important to recognize that the overall singly charged $[Pep - H + M]^+$ complex contains a divalent metal ion attached to a deprotonated peptide. The most likely site of deprotonation is the C-terminal carboxylic acid. Gross and co-workers have, however, shown that structures containing deprotonated amides can coexist, because divalent transition metal ions increase the gas phase acidity of amide N–H bonds; such structures are often required to account for several dissociations of gaseous $[Pep - H + M]^+$ ions [28].

A reaction common to all $[Pep - H + M]^+$ precursor ions studied is the abundant loss of carbon monoxide (Figs. 6 and 7). This process has a lower yield for the complexes of alkali and monovalent transition metal ions (Figs. 1–5), suggesting a selective cleavage by divalent transition metal ions. A plausible pathway for the expulsion of CO is presented in Scheme 5 and invokes a reacting configuration in which M^{2+} interacts with the deprotonated amide next to the C-terminus. Being in β-position to the C-terminal carbonyl group, this nucleophilic amide can induce the elimination of CO and hydroxide transfer to the metal ion, as shown in Scheme 5; a driving force for the reaction could be the high stability of M^{2+}–OH^- bonds, which are present in several enzymes [1,2]. Due to the low propensity of monovalent transition (or alkali) metal ions to deprotonate amides, an analogous mechanism with such metal ions would require higher energies, thus explaining the lower abundance of CO loss in the PSD spectra of their Pep complexes.

Besides losing CO, the $[Pep - H + M]^+$ adducts of des-Arg^1-bradykinin decompose to form mainly *y*-type ions that have additionally lost elements of the three possible side chains [Figs. 6(a) and 7(a)]. Such side chain cleavages have also been observed by Gross and co-workers [25,28] and Adams and co-workers [26] from anionic $[peptide - 3H + M]^-$ systems. The most abundant sequence ion in Figs. 6(a) (#4) and 7(a) (#5) corresponds to y_5^* (abbreviation for $[y_5 - 2H + M]^+$) less the entire arginine side chain (100 u); an almost equally abundant PSD product arises by loss of part of the arginine chain (85 u) from $[Pep - H + M]^+$ (#8 in both spectra). Similar to the expulsion of CO, it is possible to rationalize both these fragments via structures containing a deprotonated amide next to the C-terminus (Scheme 6). As discussed by Gross and co-workers [25], M^{2+}–N^- bonds can be cleaved homolytically; this process reduces the metal ion to the M^+ state and generates an unpaired electron at the N atom, which can now induce radical site reactions, typically α-cleavages

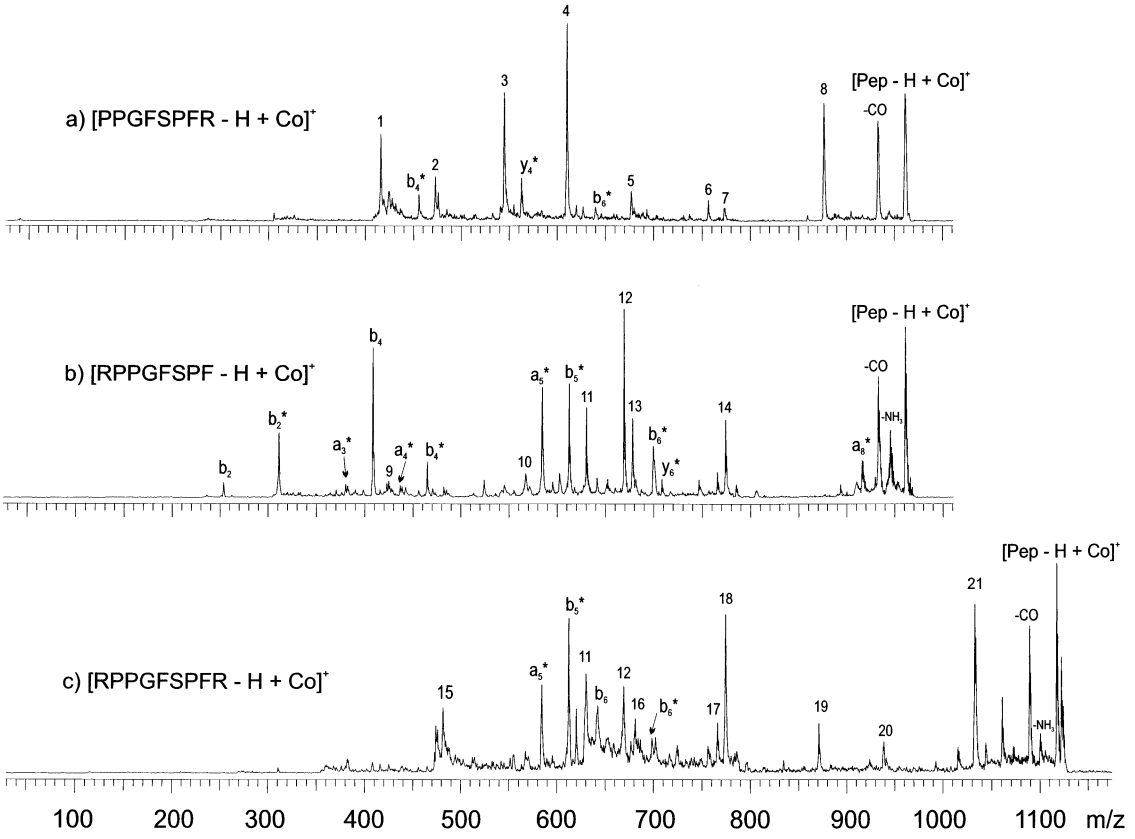

Fig. 6. PSD spectra of Co^{2+} complexes; (a) [des-Arg^1-bradykinin − H + Co]$^+$, (b) [des-Arg^9-bradykinin − H + CO]$^+$, and (c) [bradykinin − H + Co]$^+$. Peaks labeled with numbers correspond to: 1, $[y_3^* - 60]$; 2, $[b_4 + Co + O - H]$; 3, $[y_4^* - H_2O]$; 4, $[y_5^* - 100]$ (see text); 5, $[y_6^* - C_7H_7]$; 6, $[b_7^* - CH_2OH]$; 7, $[b_7 + Co + O - CH_3OH]$; 8, [precursor ion − 85] (see text); 9, $[b_3 + Co + O - H]$; 10, $[a_5^* - NH_3]$; 11, $[b_5 + Co + O]$, 12, $[b_6^* - CH_2O]$; 13, $[y_6^* - CH_2OH]$; 14, $[y_7^* - CH_2OH]$; 15, $[b_4 + Co + O - H]$; 16, $[b_6^* - H_2O]$; 17, $[y_6^* - 1]$; 18, $[y_7^* - C_7H_7]$; 19, $[y_8^* - C_7H_7]$; 20, [precursor ion − 85 − C_7H_9]; 21 [precursor ion − 85] (see text).

and γ-H transfers. γ-H-transfer from the arginine side chain of $[Pep - H + M]^+$ (Scheme 6) initiates the cleavage of CH_2=CHNHC(NH_2)=NH (85 u) from it to yield the $[Pep - H + M - 85]^+$ fragment (a radical cation). Alternatively, α cleavage in y_5^* (formed according to Scheme 3) detaches the entire arginine side chain (Scheme 6), creating $[y_5^* - 100]^+$. An additional fragment that includes the loss of elements from the arginine side chain is $[y_3^* - 60]^+$ [#1 in Figs. 6(a) and 7(a)]. Based on studies by Tang et al. [14], the 60 u neutral consists of H_2O + HN=C=NH and is characteristic of peptides containing C-terminal arginine residues (vide supra). It is important to mention at this point that all *y*-type ions observed from the M^{2+} complexes of des-Arg^1-bradykinin contain at least one phenylalanine residue, with the most intense fragment (i.e. $[y_5^* - 100]^+$) accommodating two of such residues. The high intrinsic affinity of M^{2+} to aromatic side chains, which had been documented by Gross and co-workers with smaller peptides [28], is in perfect accord with M^{2+} being a borderline Lewis acid that prefers binding at sites containing aromatic π electrons (which are borderline Lewis bases).

In contrast to des-Arg^1-bradykinin, the $[Pep - H + M]^+$ adducts of des-Arg^9-bradykinin decay to predominantly produce *a*- and *b*-type ions; when intact, these sequence ions have the composition

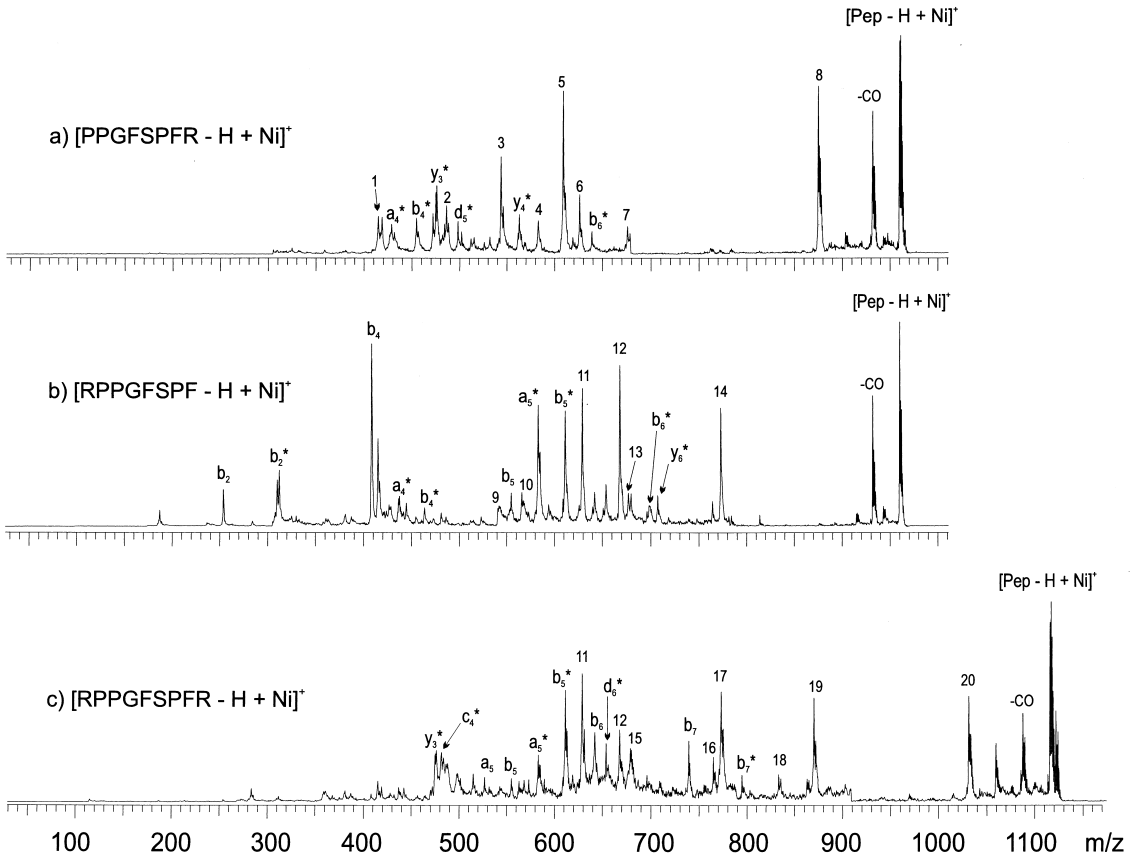

Fig. 7. PSD spectra of Ni^{2+} complexes; (a) [des-Arg^1-bradykinin − H + Ni]$^+$, (b) [des-Arg^9-bradykinin − H + Ni]$^+$, and (c) [bradykinin − H + Ni]$^+$. Peaks labeled with numbers correspond to: 1, [y_3^* − 60]; 2, [a_5^* − CO]; 3, [y_4^* − H_2O]; 4, [a_6^* − CO], 5, [y_5^* − 100]; 6, [b_6 + Ni + O − CH_2OH], 7, [y_6^* − C_7H_7]; 8, [precursor ion − 85]; 9, [PPGFS (or PGFSP) − H + Ni − H_2O]$^+$; 10, [a_5^* − NH_3]; 11, [b_5 + Ni + O]; 12, [b_6^* − CH_2O]; 13, [y_6^* − CH_2OH]; 14, [y_7^* − CH_2OH]; 15, [b_6^* − H_2O]; 16, [y_6^* − 2]; 17, [y_7^* − C_7H_7]; 18, [y_7^* − CH_2OH]; 19, [y_8^* − C_7H_7]; 20, [precursor ion − 85].

$[a_n/b_n - 2H + M]^+$ and are abbreviated as a_n^*/b_n^*, cf. Figs. 6(b) and 7(b). Consecutive fragmentation of a_n^*/b_n^* by loss of side chain elements, mainly from the Ser residue, also takes place. However, the Arg side chain eliminations observed with the des-Arg^1 analog (Scheme 6) are not detected, indicating that the latter reactions are characteristic of a C-terminal arginine. The major N-terminal fragments include a_5^*, b_5^*, $[b_5 + M + O]^+$ (#11 in both spectra; equivalent to $[b_n + M + OH]^+$ for monovalent metal ions), and $[b_6^* - CH_2O]^+$ (#12). In addition to N-terminal fragments, the PSD spectra contain two quite abundant y_n^* ions (viz. $y_{6,7}^*$ [60] that have also lost $^{\cdot}CH_2OH$ from the serine side chain (#13 and 14 in Figs. 6 and 7). The dominant b_n^* ions presumably have oxazolone structures and are generated according to Scheme 4. The b_6^* oxazolone produced this way is depicted in Scheme 7, along with a reasonable mechanism for the consecutive CH_2O elimination from the Ser side chain [52], which gives rise to the most abundant metalated sequence ion, $[b_6^* - CH_2O]^+$ (#12); note that the CH_2O loss produces an aromatic oxazole ring, providing a rationale for the high yield of $[b_6^* - CH_2O]^+$. It is again emphasized that all major metalated sequence ions contain at least one phenylalanine residue, in keeping with the high intrinsic affinity of

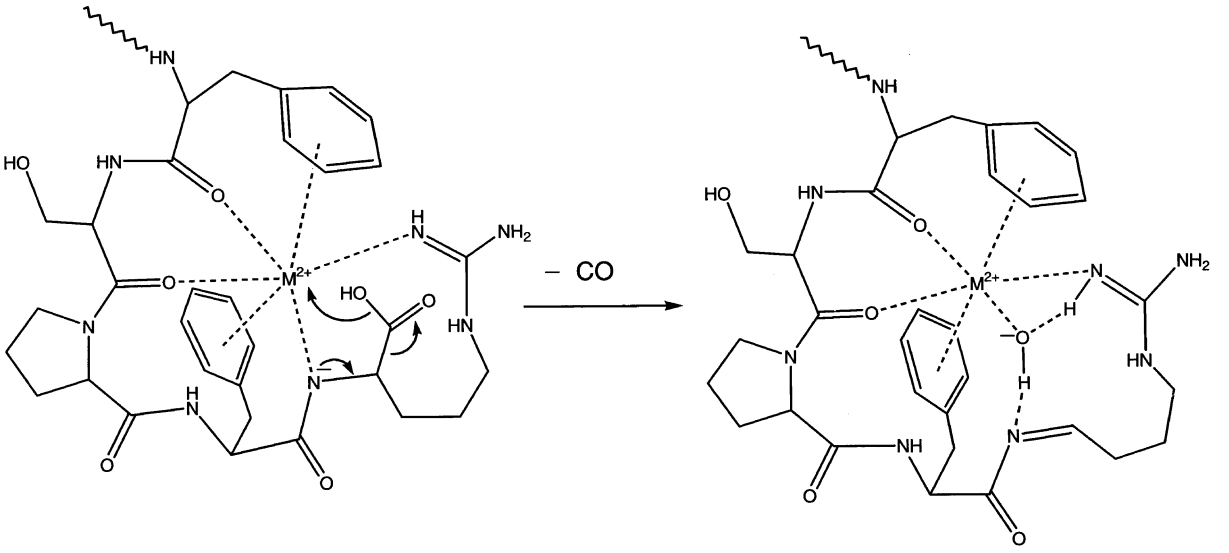

Scheme 5.

Co^{2+} and Ni^{2+} to interact with aromatic π electrons (vide supra).

A distinctive feature in the PSD spectra of the des-Arg^9-bradykinin complexes, $[RPPGFSPF - H + M]^+$, is the presence of an intense protonated b_4 fragment ion with the sequence RPPG. To form this ion, the metal-containing neutral $[FSPF - 2H^+ + M^{2+}]^0$ must be eliminated, which necessitates intramolecular proton transfer from the segment bearing the metal ion (and the charge) to the N-terminal segment emerging as the protonated species; a likely reaction path is given in Scheme 8. Several factors suggest that the sequence of des-Arg^9-bradykinin promotes such a process: (1) the highly basic N-terminal residue (R) [61] can easily deprotonate a C-terminal carboxylic acid (as shown in Scheme 8) or an amide nitrogen whose acidity has been raised by the interaction with the metal ion (vide supra); (2) the flexibility and length of the arginine side chain allow for H^+ transfer between distant residues; and, most importantly, (3) the sequences of the resulting protonated ion (RPPG) and metal-containing neutral (FSPF) bind very strongly protons (at R) and divalent transition metal ions (at F), respectively. As a result, the intramolecular proton transfer generates products that are thermodynamically favored, viz. a b_4 ion with a protonated arginine residue and a neutral fragment coordinating M^{2+} by two phenylalanine residues and two negatively charged sites. Weaker b_2 and (only with Co^{2+}) b_5 ions are also formed; their lower yield suggests inferior stabilization of H^+/M^{2+} within these ions and the respective neutral losses (as compared to that possible in the b_4 system).

The PSD spectra of the bradykinin complexes, viz. $[RPPGFSPFR - H + M]^+$, display characteristics that are partly unique and partly common to those of the two des-Arg analogs [Figs. 6(c) and 7(c)]. As with des-Arg^1-bradykinin, PSD leads to C-terminal *y*-type ions that are also missing extra side chain residues; now, however, the main fragments of this type, which are $[y_7^* - C_7H_7]^+$ [#18 in Fig. 6(c) and #17 in Fig. 7(c)] and $[y_8^* - C_7H_7]^+$ (#19 in Figs. 6 and 7), have lost the F side chain (91 u), not the R side chain (100 u). A portion of the R side chain (85 u) is still lost from the molecular ion [#21 in Fig. 6(c) and #20 in Fig. 7(c)], in analogy to des-Arg^1-bradykinin. Similar to des-Arg^9-bradykinin, N-terminal ions are also produced, with some decomposing further at the serine side chain; ions a_5^*, b_5^*, $[b_5 - 2H + M]^+$ (#11), $[b_6^* - CH_2O]^+$ (#12), and $[b_6^* - H_2O]^+$ [#16 in Fig. 6(c) and #15 in Fig. 7(c)] are readily recognized in the spectra. An important difference between Pep and

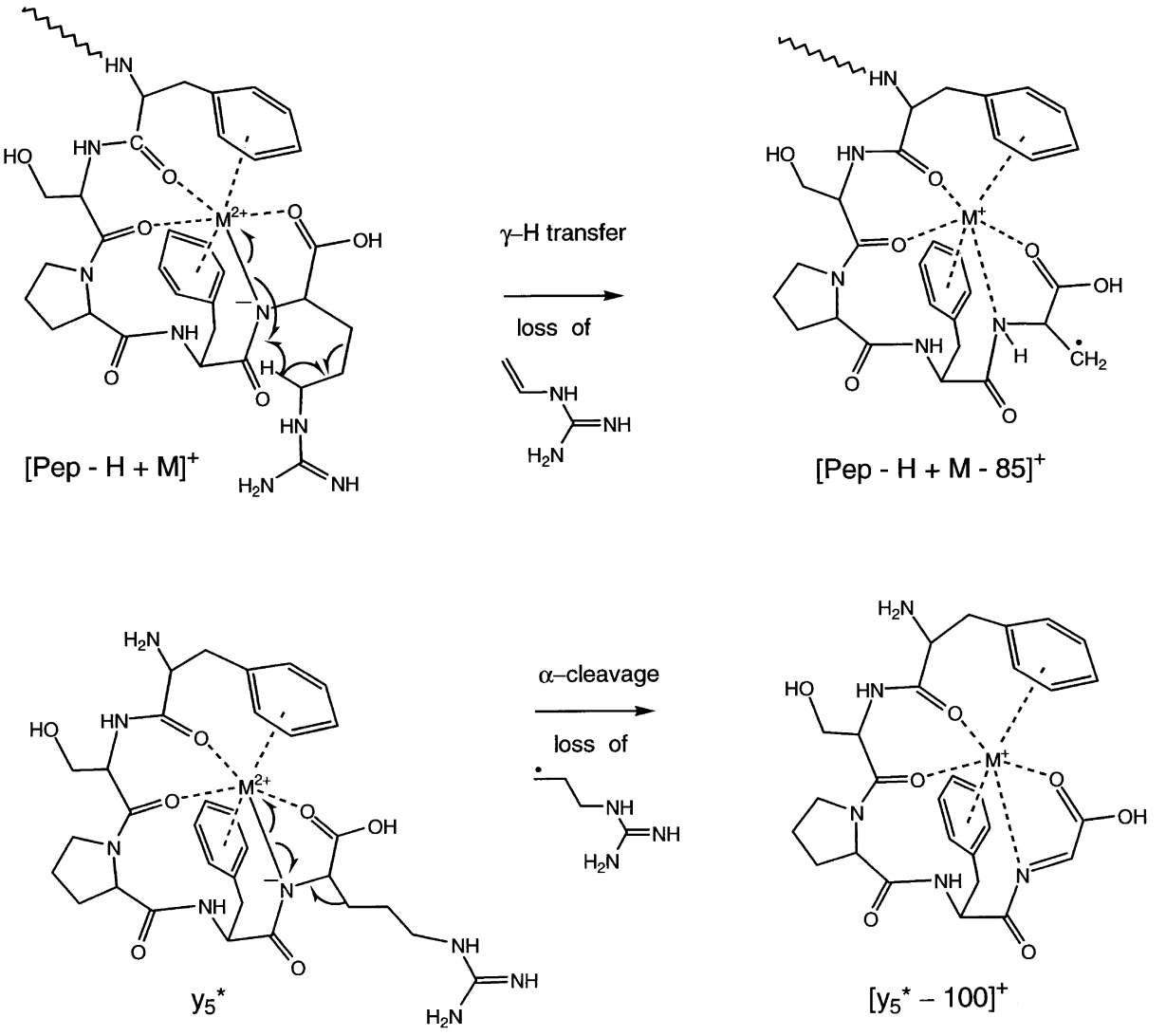

Scheme 6.

des-Arg[9]-Pep is the absence of an intense protonated b_4 (or b_5) ion in the PSD spectrum of the former; instead, weaker protonated b_6 and (only with Co^{2+}) $a_5/b_{5,7}$ are formed. The smaller fraction of non-metalated fragment ions is possibly due to the fact that now both termini possess a basic R residue, hindering intramolecular proton transfer.

3.4. PSD of [Pep − H + Zn]$^+$ ions

Similar to Co^{2+} and Ni^{2+}, Zn^{2+} is a borderline Lewis acid, favoring bonds to aromatic rings. Zn^{2+} also is, however, a closed-shell d^{10} ion, and as such it prefers tetrahedral coordination, as do Cu^+ and Ag^+. A result of these intrinsic properties is that the [Pep −

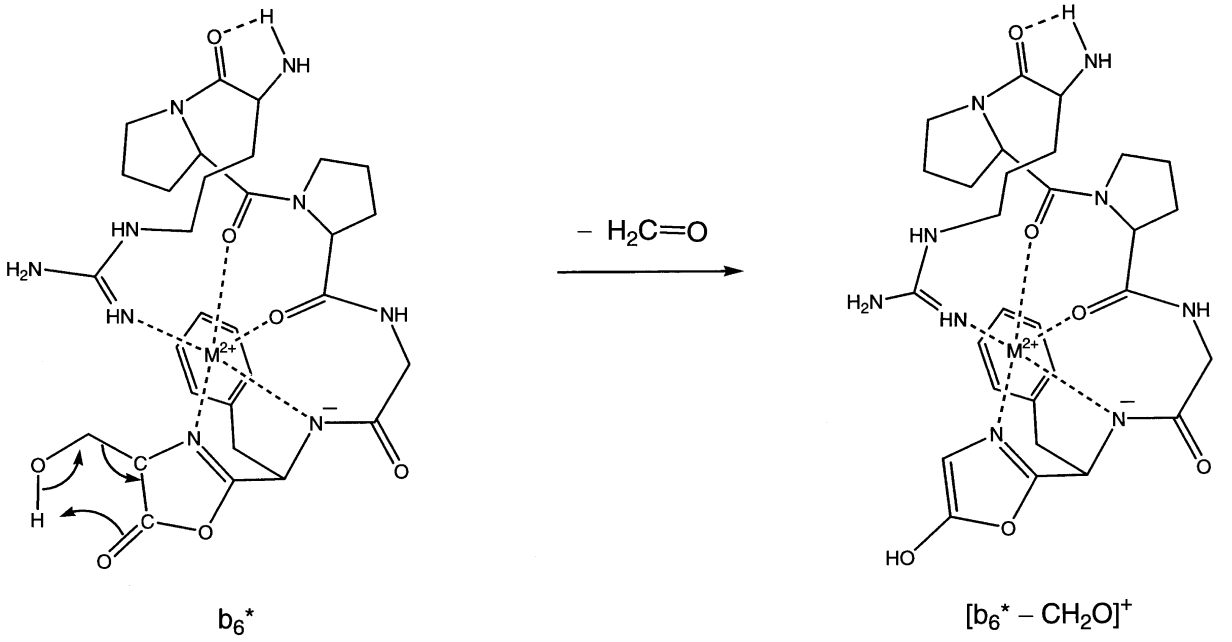

Scheme 7.

$H + Zn]^+$ complexes studied decay in a manner that contains characteristics of both the divalent $[Pep - H + Co]^+$ and $[Pep - H + Ni]^+$ and the monovalent $[Pep + Cu]^+$ and $[Pep + Ag]^+$ systems (Fig. 8). Similarities with the divalent metal ions include the abundant loss of CO from all precursor ions, the loss of an 85 u neutral from the Arg side chain from precursor ions carrying a C-terminal arginine [#7 in Fig. 8(a) and #18 in Fig. 8(c)], as well as the generation of $[y_5^* - 100]^+$ from the complex of des-Arg^1-Pep [#6 in Fig. 8(a)]. On the other hand, the Zn^{2+} complexes show a somewhat lower propensity for forming sequence ions that have also lost elements of their side chains (which is also true for the monovalent transition metal ions).

The $[Pep - H + Zn]^+$ complex of des-Arg^1-bradykinin [Fig. 8(a)] produces intense *y*-type ions, viz. y_1^*, y_3^*, y_4^*, $[y_4^* - H_2O]^+$ (#5), and the arginine immonium ion $[HN{=}CH(CH_2)_3NHC(NH_2){=}NH - H + Zn]^+$ (#2), which mimics the behavior of the Cu^+ and Ag^+ complexes. However, a significant number of N-terminal products is also generated, inter alia $b_{3,4}^*$ and $a_{4,5}^*$, pointing out that the C-terminal Arg residue does not bind Zn^{2+} as strongly as Cu^+/Ag^+ (where N-terminal fragments were much weaker).

The PSD spectrum of the $[Pep - H + Zn]^+$ complex of des-Arg^9-bradykinin [Fig. 8(b)] is dominated by intact N-terminal sequence ions, as was the case with the complexes of the monovalent transition metal ions. Additionally, sizable $[b_6^* - CH_2O]^+$ (#10), $[y_{6,7}^* - CH_2OH]^+$ (#11, 12), and protonated b_4 ions are observed, which are signatures of the corresponding Co^{2+}/Ni^{2+} complexes. The observation of C-terminal ions is in sharp contrast to the Cu^+/Ag^+ complexes, which showed exclusively N-terminal fragments; this result reiterates that Zn^{2+}–Arg bonds are weaker than Cu^+–Arg or Ag^+–Arg bonds (vide supra).

Finally, the PSD spectrum of [bradykinin − H + $Zn]^+$, Fig. 8(c), shows most (but not all) fragments present in the spectra of its des-Arg analogs. The two major PSD products are y_3^* (which is base peak for the des-Arg^1 peptide) and $[b_5 + Zn + O]^+$ (which is an important but not the most abundant ion from the des-Arg^9 peptide). It is noteworthy that several

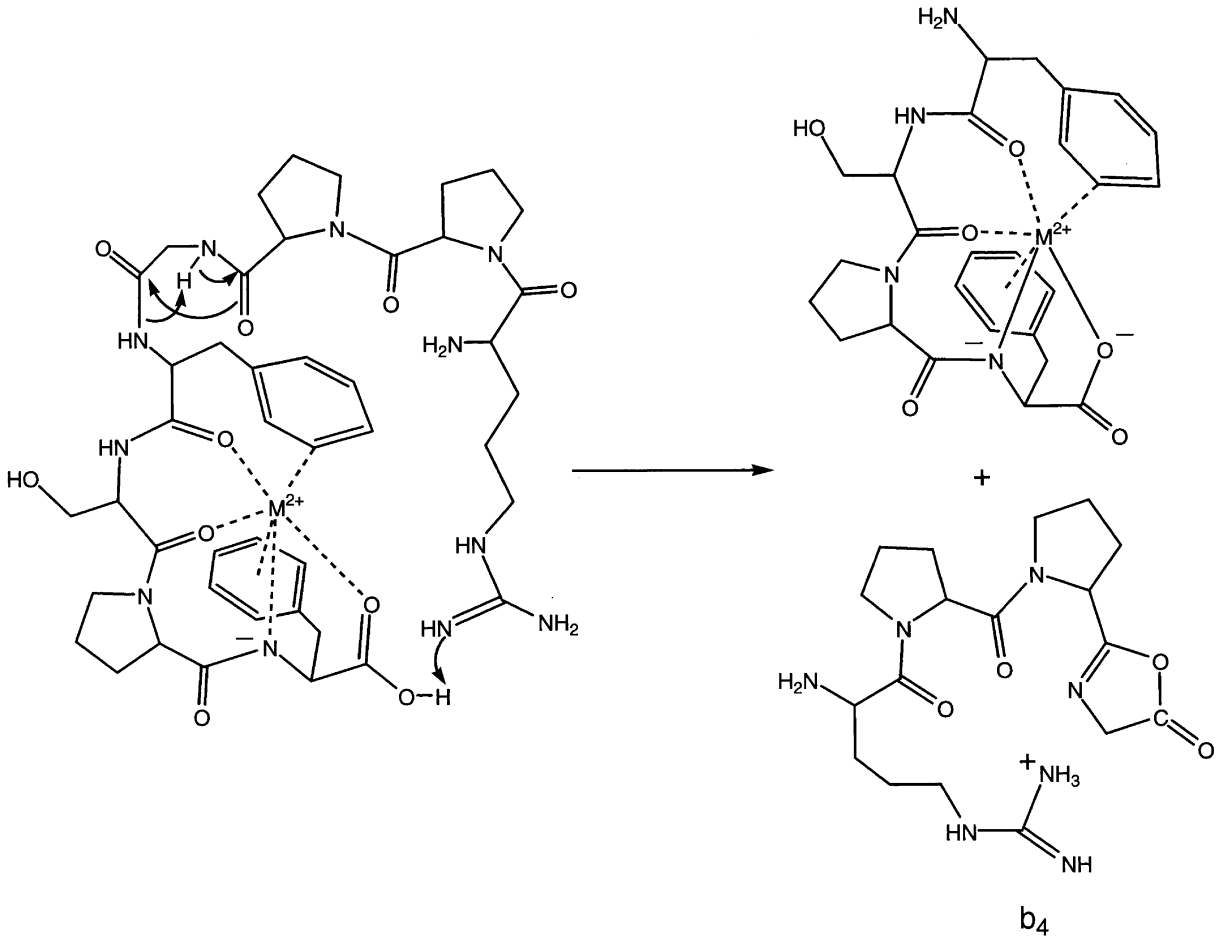

Scheme 8.

smaller fragments of the des-Arg complexes (e.g. y_1^* and b_2^* from the des-Arg^1 and des-Arg^9 complexes, respectively) are minuscule from the bradykinin complex, suggesting metal ion attachment to more central sites in bradykinin, as compared to the des-Arg derivatives.

4. Conclusions

The peptides des-Arg^1-bradykinin, des-Arg^9-bradykinin, and bradykinin interact with different classes of metal ions to form complexes whose structures reflect the intrinsic preference of each metal ion for particular coordination geometries and ligand types. The structures of the complexes influence their unimolecular reactivities; as a result, the major fragment ions observed identify the favored coordination environments of the various types of metal ions. The Na^+ and K^+ (hard Lewis acids) complexes of the peptides mainly form N-terminal fragment ions (irrespective of the position of the arginine residue), highlighting that such metal ions primarily interact with the backbone amide O atoms [45]. Based on the major fragments observed, the N-terminal sequence R (when present) PPGF is the preferred Na^+/K^+ binding domain within the peptides studied. In contrast to Na^+ and K^+, the Cs^+ adducts lead to very simple PSD spectra, dominated by the bare metal ion; this is in keeping with the

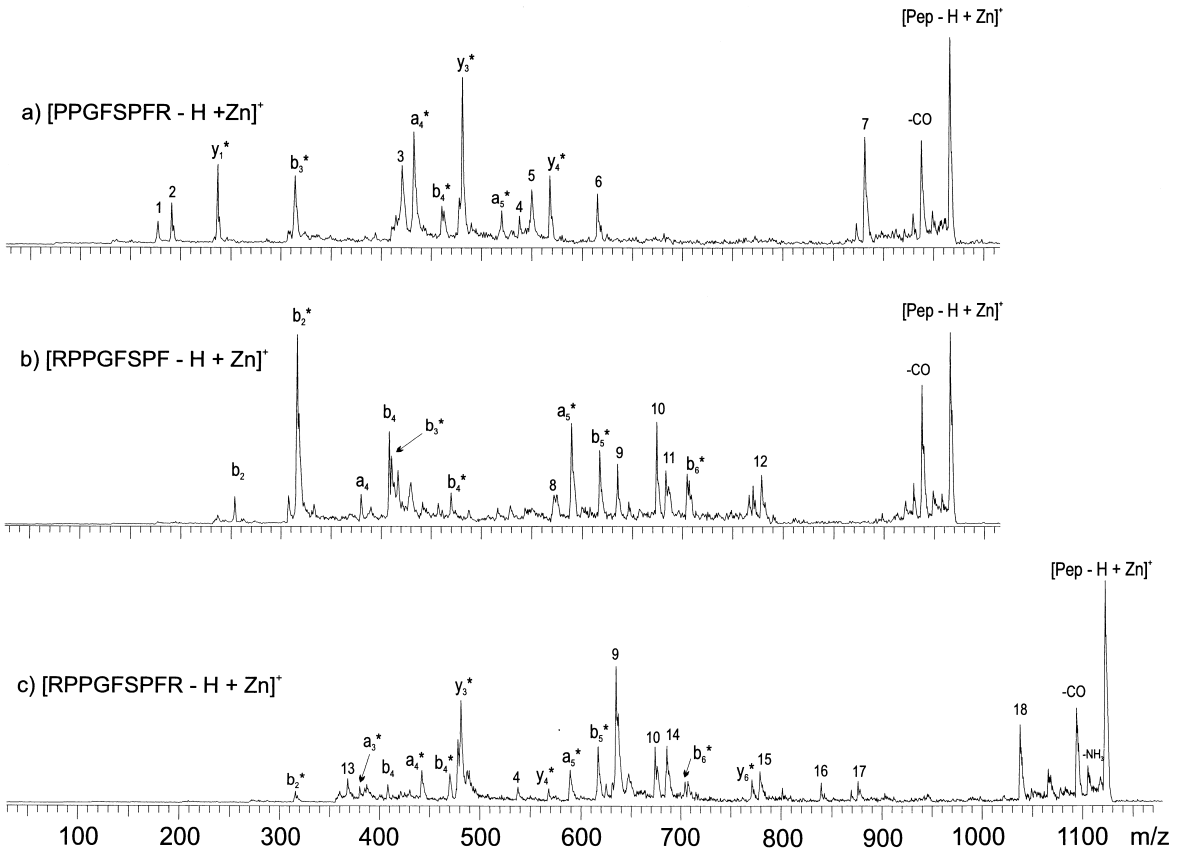

Fig. 8. PSD spectra of Zn^{2+} complexes; (a) [des-Arg^1-bradykinin − H + Zn]$^+$, (b) [des-Arg^9-bradykinin − H + Zn]$^+$, and (c) bradykinin − H + Zn]$^+$. Peaks labeled with numbers correspond to: 1, [b_1 + Zn + O − H]; 2, [HN=CH$(CH_2)_3$NHC(NH_2)=NH + Zn − H]$^+$; 3, [y_3^* − 60]; 4 [y_4^* − CH_2OH]; 5, [y_4^* − H_2O]; 6, [y_5^* − 100]; 7, [precursor ion − 85]; 8, [a_5^* − NH_3]; 9, [b_5 + Zn + O]; 10, [b_6^* − CH_2O]; 11, [y_6^* − CH_2OH]; 12, [y_7^* − CH_2OH]; 13, [a_3^* − NH_3]; 14, [b_6^* − H_2O]; 15, [y_7^* − C_7H_7]; 16, [y_7^* − CH_2OH]; 17, [y_8^* − C_7H_7]; 18, [precursor ion − 85].

larger ionic radius and decreased binding strength of this metal ion. On the other hand, Cs^+ enhances the population of zwitterionic structures within the complexes, which are detected by their unique dissociation to [d_n^* − H_2O]$^+$ ions.

Cu^+ and Ag^+ are soft, closed-shell d^{10} Lewis acids that prefer distorted tetrahedral binding to soft donor bases such as those provided by the arginine residue. The strong affinity to arginine residues is indicated by the almost exclusive formation of N- or C-terminal fragment ions from the complexes containing only one arginine at the N- or C-terminus, respectively.

The divalent transition metal ions Ni^{2+} and Co^{2+} interact preferentially with borderline Lewis bases in distorted octahedral arrangements. The major fragment ions of their complexes consequently contain at least one phenylalanine in sequences capable of providing the desired octahedral coordination. It is important to note that the Ni^{2+}/Co^{2+} complexes investigated are overall singly charged, i.e. they contain deprotonated peptides. Although the initial deprotonation site may be the acidic carboxyl terminus, the PSD fragments observed are consistent with a substantial population of deprotonated amides in the complexes. The formation of such structures is facilitated by the high intrinsic affinity of Ni^{2+}/Co^{2+} to negatively charged nitrogen atoms; the N^- sites affect

the reactivity of the complexes, by inducing eliminations from the nearby side chain, a phenomenon that had been reported previously [25]. The side chain cleavages observed suggest deprotonation at any of the available N–H groups, including those originating from Ser, Phe, and Arg. Several major fragments can be accounted for by structures where N^- resides next to the C-terminal residue (cf. Schemes 6–8), suggesting a high tendency for such an amide bond to deprotonate. Finally, Zn^{2+}, also a borderline Lewis acid, shows preference for the same ligands as Ni^{2+} and Co^{2+}; however due to its closed-shell d^{10} character, it also assumes characteristics that are found for the monovalent transition metal ions Cu^+ and Ag^+.

The present study has shown that PSD mass spectrometry can furnish valuable data on the binding of metal ions to peptides with molecular weights about 1000 u. Moreover, several of the complexes generate unique, abundant fragment ions that are particularly suitable for the detection of specific sequence motifs.

Acknowledgements

The authors gratefully acknowledge financial support from the NSF (DMR-9703946) and the University of Akron.

References

[1] S.J. Lippard, J.M. Berg, Principles of Bioinorganic Chemistry, University Science Books, Mill Valley, CA, 1994, and references therein.
[2] W. Kaim, B. Schwederski, Bioinorganic Chemistry: Inorganic Elements in the Chemistry of Life, Wiley, Chichester, 1994, and references therein.
[3] (a) L.M. Mallis, D.H. Russell, Anal. Chem. 58 (1986) 1076; (b) D.H. Russell, E.S. McGlohon, L.M. Mallis, ibid. 60 (1988) 1818.
[4] X. Tang, W. Ens, K.G. Standing, J.B. Westmore, Anal. Chem. 60 (1988) 1791.
[5] D. Renner, G. Spiteller, Biomed. Environ. Mass Spectrom. 15 (1988) 75.
[6] R.P. Grese, R.L. Cerny, M.L. Gross, J. Am. Chem. Soc. 111 (1989) 2835.
[7] J.A. Leary, T.D. Williams, G. Bott, Rapid Commun. Mass Spectrom. 3 (1989) 192.
[8] J.A. Leary, Z. Zhou, S.A. Ogden, T.D. Williams, J. Am. Soc. Mass Spectrom. 1 (1990) 473.
[9] W. Kulik, W. Heerma, Biol. Mass Spectrom. 20 (1991) 553.
[10] K.B. Tomer, L.J. Deterding, C. Guenat, Biol. Mass Spectrom. 20 (1991) 121.
[11] L.M. Teesch, J. Adams, J. Am. Chem. Soc. 113 (1991) 812.
[12] L.M. Teesch, R.C. Orlando, J. Adams, J. Am. Chem. Soc. 113 (1991) 3668.
[13] L.M. Teesch, J. Adams, Org. Mass Spectrom. 27 (1992) 931.
[14] X.-J. Tang, P. Thibault, R.B. Boyd, Org. Mass Spectrom. 28 (1993) 1047.
[15] P. Hu, M.L. Gross, J. Am. Soc. Mass Spectrom. 5 (1994) 137.
[16] S.G. Summerfield, V.C.M. Dale, D. Despeyroux, K.R. Jennings, J. Am. Chem. Soc. 117 (1995) 10093.
[17] J. Wang, R. Guevremont, K.W.M. Siu, Eur. Mass Spectrom. 1 (1995) 171.
[18] D.G. Morgan, M.M. Bursey, J. Mass Spectrom. 30 (1995) 473.
[19] J. Wang, F. Ke, K.W.M. Siu, R. Guevremont, J. Mass Spectrom. 30 (1996) 159.
[20] G. Giorgi, M. Ginanneschi, M. Chelli, A.M. Papini, F. Laschi, E. Borghi, Rapid Commun. Mass Spectrom. 10 (1996) 1266.
[21] P.T.M. Kenny, K. Nomoto, R. Orlando, Rapid Commun. Mass Spectrom. 11 (1997) 224.
[22] B. Cerda, C. Wesdemiotis, J. Am. Chem. Soc. 120 (1998) 2437.
[23] J.P. Speir, G.S. Gorman, I.J. Amster, J. Am. Soc. Mass Spectrom. 4 (1993) 106.
[24] T.W. Hutchens, M.H. Allen, Rapid Commun. Mass Spectrom. 6 (1992) 469.
[25] P. Hu, M.L. Gross, J. Am. Chem. Soc. 115 (1993) 8821.
[26] Reiter, J. Adams, H. Zhao, J. Am. Chem. Soc. 116 (1994) 7827.
[27] M.C. Sullards, J. Adams, J. Am. Soc. Mass Spectrom. 6 (1995) 608.
[28] P. Hu, C. Sorensen, M.L. Gross, J. Am. Soc. Mass Spectrom. 6 (1995) 1079.
[29] P. Hu, J.A. Loo, J. Am. Chem. Soc. 117 (1995) 11314.
[30] H. Li, K.W.M. Siu, R. Guevremont, J.C.Y.L. Blanc, J. Am. Soc. Mass Spectrom. 8 (1997) 781.
[31] I.A. Kaltashov, R.J. Cotter, W.H. Feinstone, G.W. Ketner, A.S. Woods, J. Am. Soc. Mass Spectrom. 8 (1997) 1070.
[32] O.V. Nemirovskiy, M.L. Gross, J. Am. Soc. Mass Spectrom. 9 (1998) 1285.
[33] R.W. Nelson, T.W. Hutchens, Rapid Commun. Mass Spectrom. 6 (1992) 4.
[34] T.W. Hutchens, R.W. Nelson, M.H. Allen, C.M. Li, T.-T. Yip, Biol. Mass Spectrom. 21 (1992) 151.
[35] S.T. Fountain, H. Lee, D.M. Lubman, Rapid Commun. Mass Spectrom. 8 (1994) 407.
[36] P.-C. Liao, J. Allison, J. Mass Spectrom. 30 (1995) 408.
[37] A.S. Woods, J.C. Buchsbaum, T.A. Worrall, J.M. Berg, R.J. Cotter, Anal. Chem. 67 (1995) 4462.
[38] T. Wyttenbach, G. v. Helden, M.T. Bowers, J. Am. Chem. Soc. 118 (1996) 8355.
[39] A. Wattenberg, H.-D. Barth, B. Brutschy, J. Mass Spectrom. 32 (1997) 1350.

[40] B. Salih, C. Masselon, R. Zenobi, J. Mass Spectrom. 33 (1998) 994.
[41] S.J. Shields, B.K. Bluhm, D.H. Russell, Proceedings of the 46th ASMS Conference on Mass Spectrometry and Allied Topics, Orlando, FL, 31 May–4 June 1998, p. 29.
[42] B. Spengler, J. Mass Spectrom. 32 (1997) 1019.
[43] P. Roepstorff, J. Fohlman, Biomed. Mass Spectrom. 11 (1984) 601.
[44] S.A. Martin, R.S. Johnson, C.E. Costello, K. Biemann, in The Analysis of Peptides and Proteins by Mass Spectrometry, C.J. McNeal (Ed.), Wiley, Chichester, 1988, p. 135.
[45] O.V. Nemirovskiy, M.L. Gross, J. Am. Soc. Mass Spectrom. 9 (1998) 1020.
[46] (a) P. Schnier, W.D. Price, R.A. Jockusch, E.R. Williams, J. Am. Chem. Soc. 118 (1996) 7178; (b) W.D. Price, R.A. Jockusch, E.R. Williams, ibid. 119 (1997) 11988.
[47] E.R. Williams, E.F. Strittmatter, R.A. Jockusch, R.L. Wong, presented at the 47th ASMS Conference on Mass Spectrometry and Allied Topics, Dallas TX, 13–17 June 1999, TOD 10:35.
[48] C. Wesdemiotis, B.A. Cerda, presented at the 47th ASMS Conference on Mass Spectrometry and Allied Topics, Dallas TX, 13–17 June 1999, TOD 10:55.
[49] B.A. Cerda, C. Wesdemiotis, J. Am. Chem. Soc. 117 (1995) 9734.
[50] B.A. Cerda, C. Wesdemiotis, Int. J. Mass Spectrom. 185/186/187 (1999) 107.
[51] S. Hoyau, G. Ohanessian, J. Am. Chem. Soc. 119 (1997) 2016.
[52] P. Hu, M.L. Gross, J. Am. Chem. Soc. 114 (1992) 9153.
[53] (a) T. Yalcin, I.G. Csizmadia, M.B. Peterson, A.G. Harrison, J. Am. Soc. Mass Spectrom. 7 (1996) 233; (b) M.J. Nold, C. Wesdemiotis, T. Yalcin, A.G. Harrison, Int. J. Mass Spectrom. Ion Processes 164 (1997) 137.
[54] V.W.-M. Lee, H. Li, T.-C. Lau, K.W.M. Siu, J. Am. Chem. Soc. 120 (1998) 7302.
[55] V.W.-M. Lee, H. Li, T.-C. Lau, R. Guevremont, K.W.M. Siu, J. Am. Soc. Mass Spectrom. 9 (1998) 760.
[56] G. Bojesen, T. Breindahl, U. Andersen, Org. Mass Spectrom. 28 (1993) 1448.
[57] J.S. Klassen, S.G. Anderson, A.T. Blades, P. Kebarle, J. Phys. Chem. 100 (1996) 14218.
[58] S. Hoyau, K. Norman, T.B. McMahon, G. Ohanessian, J. Am. Chem. Soc., in press.
[59] Estimated from the Na^+ affinity of N-acetyl arginine (203 kJ mol^{-1}; unpublished results, this laboratory) assuming that the differences in Na^+ affinity between glycine and N-acetyl glycine (5 kJ mol^{-1} [22]) and between arginine and N-acetyl arginine are comparable.
[60] With the divalent transition metal ions, *y*-type cleavages also occur at the C-terminal side of internal proline residues. In such cases, the migrating H atom (cf. Scheme 3) probably originates from the N-terminus. The higher yield of such remote H transfers in M^{2+} complexes could be due to the increased acidity of their N–H bonds.
[61] Z. Wu, C. Fenselau, Rapid Commun. Mass Spectrom. 6 (1992) 403.